Geological Magazine

www.cambridge.org/geo

Original Article

Cite this article: Zhang ZT and Sun YD (2023) The Ladinian–Carnian conodont fauna at Yize, Yunnan, southwestern China, with implications for conodont palaeoecology and palaeogeography. *Geological Magazine* **160**: 776–793. https://doi.org/10.1017/S0016756822001236

Received: 25 June 2022
Revised: 15 November 2022
Accepted: 22 November 2022
First published online: 6 February 2023

Keywords:
Late Triassic; biostratigraphy; conodont palaeoecology; Zhuganpo Formation

Author for correspondence:
Yadong Sun,
Email: yadong.sun@cug.edu.cn

The Ladinian–Carnian conodont fauna at Yize, Yunnan, southwestern China, with implications for conodont palaeoecology and palaeogeography

Zaitian Zhang[1,2,3] and Yadong Sun[2,4]

[1]Wuhan Centre, China Geological Survey, Wuhan 430205, People's Republic of China; [2]State Key Laboratory of Biogeology and Environmental Geology, China University of Geosciences (Wuhan), Wuhan 430074, People's Republic of China; [3]State Key Laboratory of Palaeobiology and Stratigraphy, Nanjing Institute of Geology and Palaeontology, CAS, Nanjing 210008, People's Republic of China and [4]GeoZentrum Nordbayern, Universität Erlangen-Nürnberg, Schlossgarten 5, Erlangen 91054, Germany

Abstract

Subdivisions of Ladinian–Carnian boundary beds and the lower Carnian strata in South China are challenging owing to a paucity of west Tethyan ammonoids. We investigated a conodont fauna in a continuous section at Yize in eastern Yunnan Province to provide a biostratigraphic solution. Five genera and 24 conodont species are recognized, and five conodont zones are established. The zones are, in ascending order, the *Paragondolella inclinata* Zone, the *Quadralella polygnathiformis* Zone, the *Quadralella praelindae* Zone, the *Quadralella auriformis* Zone and the *Quadralella robusta* Zone. The Ladinian–Carnian boundary is provisionally defined by the first occurrences of *Quadralella polygnathiformis* and *Quadralella intermedia* in the cherty limestone member of the Zhuganpo Formation. Regional correlations via conodont biostratigraphy indicate that the Zhuganpo Formation is probably diachronous, with a maximal range spanning the upper Ladinian to the lower Carnian. Amongst all common late Ladinian – early Carnian conodont genera, *Paragondolella*, *Quadralella* and *Mazzaella* are probably cosmopolitan. *Budurovignathus* was restricted to a few basins and probably preferred offshore or deep-water environments.

1. Introduction

The Middle and Late Triassic were critical times in evolution. The global ecosystems recovered fully from the end-Permian mass extinction and started a full radiation both in the ocean and on land (Chen & Benton, 2012; Sun *et al.* 2012; Benton *et al.* 2013, 2014; Marshall, 2019). The marine realm saw the onset of the Mesozoic marine revolution, accompanied by an increase in predation pressure in an increasingly complex marine food web (Vermeij, 1977; Harper *et al.* 1998; Benton *et al.* 2014; Kelley & Pyenson, 2015; Tackett, 2016). The environmental, biotic and climatic changes have been intensively studied in this interval (e.g. Mutti & Weissert, 1995; Wang *et al.* 2008; Stefani *et al.* 2010; Benton *et al.* 2013; Trotter *et al.* 2015; Tanner, 2018; Sun *et al.* 2020). However, lining up key evolutionary events with palaeoenvironmental changes at a global scale requires a robust biostratigraphic framework and high precision supra-regional correlation, which remain challenging in many cases (e.g. Kozur, 2003; Mundil *et al.* 2010; Chen *et al.* 2015; Shen & Zhang, 2017; Rigo *et al.* 2018; Tong *et al.* 2019; Gradstein *et al.* 2020).

The Global Stratotype Section and Point for the base of the Carnian Stage is defined by the first appearance datum (FAD) of the ammonoid *Daxatina canadensis* at Prati di Stuores in NE Italy (Mietto *et al.* 2012). Correlations between the western Tethys and North America for the Ladinian–Carnian boundary (L-CB) beds are well resolved (Mietto & Manfrin, 1995; Orchard & Tozer, 1997; Gallet *et al.* 1998; Balini *et al.* 2000, 2010; Mietto *et al.* 2007, 2012; Orchard, 2007). However, correlating time-equivalent beds in the eastern and western Tethys has proven challenging. This is largely because the biostratigraphic definition of the L-CB in South China remains ambiguous owing to paucities of the ammonoids *Daxatina canadensis* and associated *Trachyceras* species (Tong *et al.* 2019). Several options were proposed, and some led to discrepant solutions (e.g. Xu *et al.* 2003; Sun *et al.* 2005; Zou *et al.* 2015).

A common practice is to define the L-CB using the FAD of '*Paragondolella*' (*P.*) *polygnathiformis*, which was ratified as the secondary auxiliary marker for the basal Carnian at Prati di Stuores (Yang *et al.* 1995; Sun *et al.* 2005; Mietto *et al.* 2012; Muttoni *et al.* 2014; Lehrmann *et al.* 2015). However, the FAD of *P. polygnathiformis* is difficult to define in practice, and large ontogenetic variation within the species hinders the resolution of this issue further (e.g. Koike, 1982; Koike *et al.* 1991; Orchard & Balini, 2007; Orchard, 2010; Chen & Lukeneder, 2017; Jiang *et al.* 2018). Therefore, additional markers for the L-CB are in urgent need.

Subdividing Carnian strata is a difficult task. Conodont zonation, especially in the lower Carnian (Julian), varies significantly in different regions (Koike, 1979; Kozur, 1980*a*, 2003; Budurov *et al.* 1985; Orchard & Tozer, 1997; Chen *et al.* 2015; Rigo *et al.* 2018; Yamashita *et al.* 2018). This is partly due to few studies being carried out and partly due to an increase in endemism in conodonts since late Middle Triassic time (e.g. Budurov *et al.* 1985; Chen *et al.* 2015). In North America, two conodont zones, namely the *Neospathodus newpassensis* Zone and the *P. polygnathiformis* Zone, were initially established for the lower Carnian in Nevada and British Columbia (Sweet *et al.* 1971). The *Metapolygnathus* (*Me.*) *polygnathiformis* Zone and the *P. inclinata–Mosherella* assemblage zone (AZ) were summarized for the lower Carnian in the Western Canada Sedimentary Basin (Orchard & Tozer, 1997). Later, the *P. inclinata* Zone (which consisted of the *P. sulcata* Subzone and the *Me. acuminata* Subzone), the *Me. intermedia* Zone and the *Me. tadpole* Zone were recognized in British Columbia (Orchard, 2007). In the western Tethys, three conodont zones, namely, the *Carinella diebeli* AZ, the *Gladigondolella* (*G.*) *tethydis* AZ and the *Gondolella polygnathiformis* AZ were established for the upper Ladinian to the lower Carnian in the Salzkammergut region of the North Calcareous Alps (Krystyn, 1980). The *P. foliata* range zone (RZ) and the *P. polygnathiformis* interval zone (IZ) were established based on collections from the Alps, Dinarides, Balkans and Himalayas (Budurov & Sudar, 1990). Later, five conodont zones, namely, the *Budurovignathus* (*B.*) *mostleri* IZ, the *Me. tadpole* IZ, the *Me. auriformis* IZ, the *Me. carnica* RZ and the *G. tethydis* IZ were recognized in the North Calcareous Alps and southwestern Turkey in the lower Carnian (Gallet *et al.* 1994). Rigo *et al.* (2018) proposed a new lower Carnian conodont scheme for the western Tethys, consisting of the *P. polygnathiformis* IZ, the *Mazzaella (Ma.) carnica* IZ and the *P. praelindae* IZ. In the Panthalassa Ocean, two zones, namely, the *Neogondolella (N.) foliata* Zone and *N. polygnathiformis* Zone, were summarized for the L-CB interval in Japan (Koike, 1979). In central Japan, only the *P. tadpole* IZ was initially established for the lower Carnian (Yamashita *et al.* 2018). This was later revised to the *Ma. carnica* Zone and the *P. praelindae* Zone in the same section (Tomimatsu *et al.* 2021). In addition, the *Quadralella* (*Q.*) *tadpole* – *G. malayensis* AZ was established in Kamura in southern Japan for the lower Carnian (Zhang *et al.* 2019).

Much progress has been made in the Carnian conodont biostratigraphy in South China (e.g. Wang *et al.* 1998, 2008; Yang *et al.* 2002; Sun, Z. Y. *et al.* 2005, 2016; Jin *et al.* 2018). Early studies only recognized two conodont zones, the *B. diebeli* Zone and the *P. polygnathiformis* Zone, for the entire Carnian (Yao, 1987; Lai & Mei, 2000). The *N. polygnathiformis* – *N. maantangensis* AZ, *N. polygnathiformis* – *N. tadpole* AZ and *N. polygnathiformis* Zone were established by Yang *et al.* (1995) in Guizhou. Yang *et al.* (1999) noticed that conodont assemblages vary with depositional settings and established the *B. diebeli* – *P.* sp. A AZ, the *P. polygnathiformis* Zone and the '*Epigondolella*' *nodosa* Zone for basinal environments and the *P. polygnathiformis* – *P. maantangensis* AZ, the *P. polygnathiformis* – *P. tadpole* AZ and the *P. polygnathiformis* Zone for platform environments (Yang *et al.* 1999; Wang & Wang, 2016). Y. D. Sun *et al.* (2016) identified the *P. foliata* – *Q. polygnathiformis* AZ, the *Q. polygnathiformis noah* AZ and the *Q.* ex gr. *carpathica* AZ in a carbonate ramp section in Guizhou. Zhang *et al.* (2018*a*) summarized eight conodont zones in southwestern China: the *P. foliata* Zone, the *Q. polygnathiformis* Zone, the *Q. tadpole* Zone, the *Q. praelindae* Zone, the *Q.* aff. *auriformis* Zone, the *Q. robusta* Zone, the *Q. noah* Zone and the *Q.* ex gr. *carpathica* Zone. Jiang *et al.* (2019) identified the *Ma. carnica* RZ in northern Sichuan.

The subdivision of the Middle and Upper Triassic strata into substages or finer levels is a longstanding conundrum in South China. To address this issue, we carried out a study in a newly excavated section in eastern Yunnan Province. Here, we define the L-CB in the Zhuganpo Formation (Fm) by using the first occurrence (FO) of *Q. polygnathiformis* and the FO of *Q. intermedia*, providing a practical solution for the L-CB definition in the region. A new conodont biostratigraphic framework is established, and the zones can be well correlated to other regions. Our study also reveals that the conodont fauna from southwestern China shows mixed morphological features compared to their North American and western Tethyan counterparts.

2. Geological setting

The South China Block has been a classic area for Triassic research. It was located in the northern low latitudes in the eastern Palaeo-Tethys during Late Triassic time and consisted of the Yangtze Platform, the Cathaysian Platform and the Nanpanjiang Basin (Fig. 1; Yin & Peng, 2000). Marine carbonates with diverse facies were extensively developed in the region during Early Triassic time. The carbonate platform continued to shrink toward Late Triassic time, partly due to the Indosinian Orogeny. Most Middle to Upper Triassic carbonate successions were deposited on the southwestern margin of the Yangtze Platform and sparsely in the Nanpanjiang Basin. The studied Yize section is located near Changdi town in Luoping city, Yunnan Province (Fig. 1), palaeogeographically belonging to the Upper Yangtze Platform.

The Yize section was freshly exposed along a hillside quarry. The measured section is 95 m in thickness and consists of the Zhuganpo and the Wayao (also known as Xiaowa) formations. The measured Zhuganpo Fm is ~90 m in thickness and is dominated by bioturbated carbonates. The unit is characterized by three distinct lithological associations. They are, in ascending order, the fine-laminated limestone member, the cherty limestone member and the nodular limestone member. The overlying Wayao Fm is ~5 m in thickness, comprising thin- to medium-bedded sandstones and mudstones (Figs 2, 3).

3. Materials and methods

The study section was logged in detail in the field and systematically sampled for conodonts with a resolution of ~1–3 m. Forty-three carbonate samples, each weighing 7–9 kg, were collected. All samples were crushed into 1–2 cm^3 rock chips and dissolved in diluted acetic acid (~8 vol. %). The undissolved residuals were wet-sieved and dried at room temperature. The heavy fractions were separated using a lithium and sodium heteropolytungstate heavy liquid (density 2.80 g cm^{-3}). Conodont elements were picked out under a binocular microscope. A total of 1234 conodont (989 P_1 and 245 ramiform) elements were recovered from 37 samples. Selected specimens were imaged using a scanning electron microscope (SEM) at the China University of Geosciences (Wuhan).

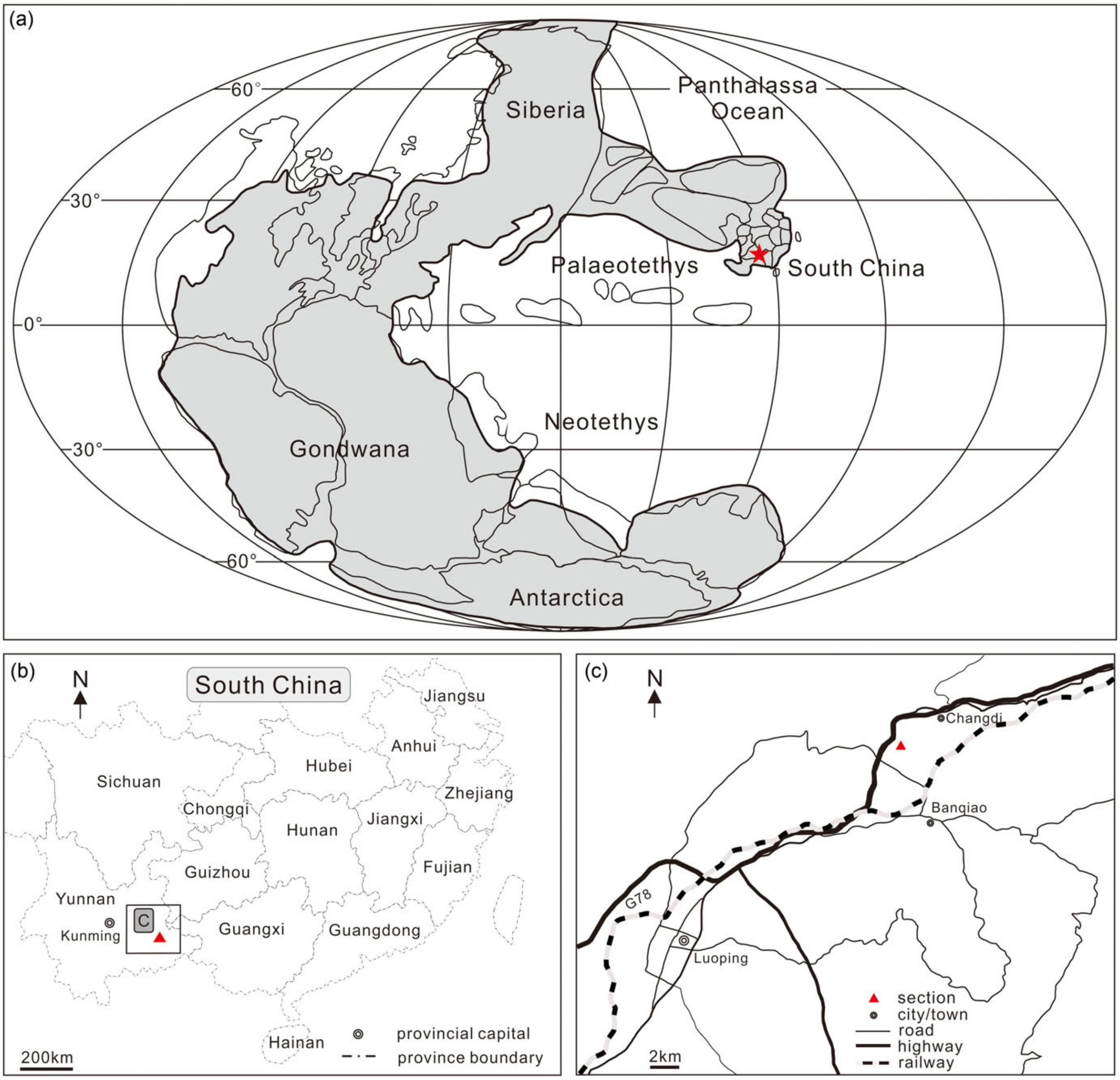

Fig. 1. (Colour online) The palaeogeographical and present-day location maps of the study section. (a) Palaeogeographical map during Carnian time (modified from Sun *et al*. 2019). (b, c) Present-day location maps of the Yize section.

4. Conodont biostratigraphy

Five conodont zones are established and described below in ascending order. Reported conodont taxa and their ranges are shown in Figure 3. Note that some genera and species are revised from their original binomial nomenclature and reassigned in accordance with the latest taxonomic studies and rules of the International Code of Zoological Nomenclature (e.g. Orchard, 2007, 2013; Chen *et al*. 2015; Kiliç *et al*. 2015, 2017; Chen & Lukeneder, 2017). For a better description of the stratigraphic context, we use stage and substage nomenclature in the following sections.

4.a. *Paragondolella inclinata* Zone

Lower limit: not defined.
Upper limit: FO of *Q. polygnathiformis*.
Associated taxa: *P. inclinata*, *Q. acuminata* (= *Me. acuminatus* in Orchard, 2007) and *Q. lobata* (= *Me. lobatus* in Orchard, 2007).

The *P. inclinata* Zone ranges from the 13.5 m to the 29.4 m level at Yize. This zone represents the last Ladinian conodont zone in South China and British Columbia (Orchard & Tozer, 1997; Orchard, 2007; Lehrmann *et al*. 2015). The zonal species is cosmopolitan ranging from the lower Longobardian to the upper Julian

Fig. 2. (Colour online) Field photographs of the study section at Yize, Yunnan Province, South China. (a) Overview of the studied section, showing the outcrop of the Zhuganpo and the Wayao formations. (b) Photo showing the fine-laminated limestones in the lower Zhuganpo Fm. (c, d) Photos showing the cherty limestone member of the Zhuganpo Fm. (e) Photo showing the thin- to medium-bedded sandstones and mudstones of the lower Wayao Fm.

(Gallet *et al.* 1998; Orchard, 2007; Rigo *et al.* 2007; Lein *et al.* 2012; Chen *et al.* 2015; Zhang *et al.* 2017). Morphologically, the species represents a transitional form from *P. excelsa* and *P. foliata* (Kovács, 1983) (Fig. 4).

In British Columbia, *Q. acuminata* and *Q. lobata* were identified in the *P. inclinata* Zone and the *Q. intermedia* Zone, respectively. Both species typically represent the Longobardian to Julian elements (Orchard, 2007). *Q. acuminata* and *Q. lobata* are also known in the Zhuganpo Fm from Guizhou and Yunnan in southwestern China as well as in Japan (Zhang *et al.* 2017, 2018*b*, 2019).

4.b. *Quadralella polygnathiformis* Zone

Lower limit: FO of *Q. polygnathiformis*.
Upper limit: FO of *Q. praelindae*.
Associated taxa: *P. foliata*, *P. inclinata*, *Q. acuminata*, *Q. intermedia* (= *Me. intermedius* in Orchard, 2007), *Q. jiangyouensis*, *Q. langdaiensis*, *Q. lobata*, *Q. maantangensis*, *Q.* aff. *polygnathiformis magna*, *Q.* spp., *Q. shijiangjunensis*, *Q. tadpole*, *Q. wanlanensis* and *Q. yongyueensis*.

The *Q. polygnathiformis* Zone ranges from the 29.4 m to the 47.1 m level at Yize. This zone was widely accepted as the first

https://doi.org/10.1017/S0016756822001236 Published online by Cambridge University Press

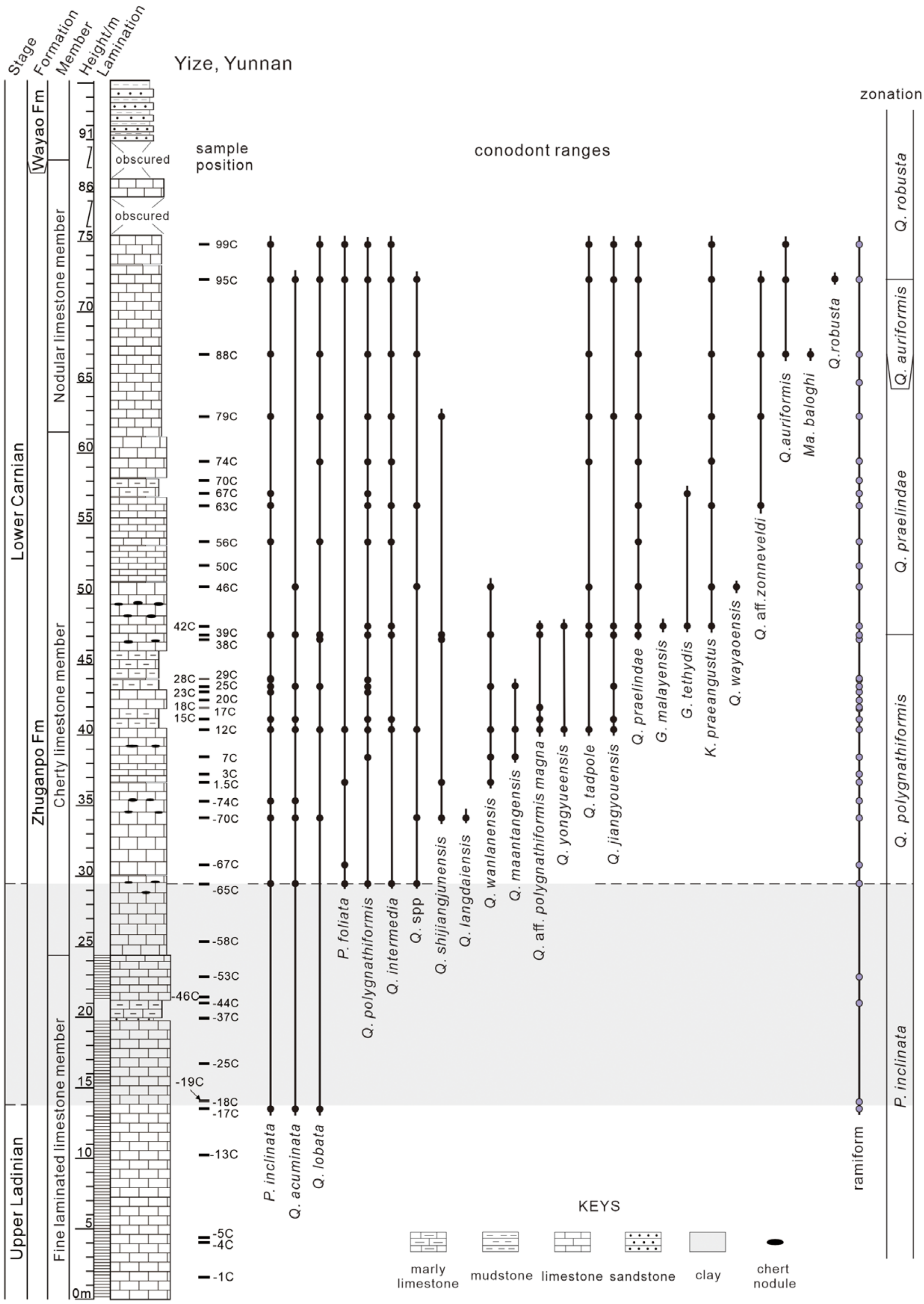

Fig. 3. Log of the Yize section, showing sample positions, conodont occurrences and zonation.

https://doi.org/10.1017/S0016756822001236 Published online by Cambridge University Press

Fig. 4. SEM photographs of conodonts from the Ladinian to Carnian strata at Yize. Scale bar = 200 μm. a – upper view; b – lateral view; c – lower view. 1 – *Q. polygnathiformis* (Budurov & Stefanov, 1965), YZ-(-65)-001; 2 – *Q. intermedia* (Orchard, 2007), YZ-(-65)-014; 3 – *Q. polygnathiformis* (Budurov & Stefanov, 1965), YZ-12-1-014; 4 – *Q. jiangyouensis* (Wang & Dai, 1981), YZ-25-003; 5 – *Q. polygnathiformis* (Budurov & Stefanov, 1965), YZ-(-65)-015; 6 – *Q. polygnathiformis* (Budurov & Stefanov, 1965), YZ-88-1-36; 7 – *Q.* aff. *polygnathiformis magna* (Igo, 1989), YZ-18-001; 8 – *Q. polygnathiformis* (Budurov & Stefanov, 1965), YZ-12-1-013; 9 – *Q.* aff. *polygnathiformis magna* (Igo, 1989), YZ-12-2-001; 10 – *Q. maantangensis* (Dai & Tian *in* Tian *et al*. 1983), YZ-25-001; 11 – *P. inclinata* (Kovács, 1983), YZ-25-002; 12 – *P. inclinata* (Kovács, 1983), YZ-28-001; 13 – *K. praeangustus* (Kozur, Mirăuta & Mock *in* Kozur, 1980*b*), YZ-42-020; 14 – *Q. polygnathiformis* (Budurov & Stefanov, 1965), YZ-42-026; 15 – *Q. intermedia* (Orchard, 2007), YZ-79-017; 16 – *Q. intermedia* (Orchard, 2007), YZ-63-005; 17 – *Q. polygnathiformis* (Budurov & Stefanov, 1965), YZ-63-007; 18 – *Q. intermedia* (Orchard, 2007), YZ-79-009; 19 – *Q. intermedia* (Orchard, 2007), YZ-95-1-003; 20 – *Q.* sp., YZ-63-008; 21 – *Q. jiangyouensis* (Wang & Dai, 1981), YZ-79-026; 22 – *Q. tadpole* (Hayashi, 1968), YZ-95-1-006; 23 – *Q. robusta* Zhang, Sun & Lai *in* Zhang *et al*. 2018*b*, YZ-95-2-022; 24 – *Q. polygnathiformis* (Budurov & Stefanov, 1965), YZ-95-1-005.

Carnian conodont zone (e.g. Orchard & Tozer, 1997; Kozur, 2003; Rigo *et al.* 2018; Tong *et al.* 2019). The FAD of *Q. polygnathiformis* is the secondary marker to define the base of the Carnian (Mietto *et al.* 2012). *Q. polygnathiformis* ranges typically from the lower Julian to the lower Tuvalian and may extend to the upper Tuvalian (e.g. Gallet *et al.* 1994; Rigo *et al.* 2007, 2018; Muttoni *et al.* 2014; Chen *et al.* 2015). Some studies implied that *Q. polygnathiformis* might appear in older strata below the FAD of *Daxatina canadensis* (Krystyn *et al.* 2004; Orchard, 2007, 2010; Mietto *et al.* 2012). The essential feature of this species is the geniculation(s)/abrupt step(s) at the anterior margins, which differs from Ladinian holdovers. However, *Q. polygnathiformis* may show large morphological variations in the posterior platform during different ontogenetic stages (e.g. Orchard & Balini, 2007; Chen & Lukeneder, 2017) (Fig. 5).

P. foliata is also a cosmopolitan species and differs from *P. inclinata* by having a straight basal edge before the basal cavity (Koike, 1982; Kovács, 1983; Muttoni *et al.* 2014; Zhang *et al.* 2017). The species ranges from the Longobardian 3 to the Tuvalian 1 (Lein *et al.* 2012; Muttoni *et al.* 2014), but is most common in the Julian (Rigo *et al.* 2007; Zhang *et al.* 2017).

Q. intermedia was first identified in the *Frankites sutherlandi* ammonoid zone in British Columbia (Orchard, 2007) and has been reported in Nevada and southwestern China (Orchard, 2007; Orchard & Balini, 2007; Zhang *et al.* 2017, 2018*b*). The FO of *Q. intermedia* has been used as an effective marker for the base of the Carnian in British Columbia because of its co-occurrence with *Daxatina canadensis* and its unambiguous evolution lineage (Orchard, 2007). This species is thought to derive from *Q. acuminata* through further reduction in the anterior platform (Orchard, 2007). Reduction in the anterior platform and a narrowly rounded posterior end are key diagnostic features of *Q. intermedia* that differentiate the species from *Q. polygnathiformis* (Orchard, 2007; Orchard & Balini, 2007).

Q. tadpole is characterized by its tadpole-shaped platform and was widely reported in the Tethys, North America and Panthalassa (e.g. Hayashi, 1968; Gallet *et al.* 1994; Orchard, 2007; Mietto *et al.* 2012; Zhang *et al.* 2017, 2019). This species commonly occurred in the Julian and disappeared in the Tuvalian (Rigo *et al.* 2007; Chen *et al.* 2015; Kiliç *et al.* 2017; Tomimatsu *et al.* 2021) (Fig. 6).

Q. jiangyouensis, *Q. langdaiensis*, *Q. maantangensis*, *Q. shijiangjunensis* and *Q. yongyueensis* are only reported from South China to date (Wang & Dai, 1981; Tian *et al.* 1983; Yang *et al.* 2002; Sun, 2006; Sun, Y. D. *et al.* 2016; Zhang *et al.* 2017, 2018*b*). *Q.* aff. *maantangensis* was reported in central Japan (Tomimatsu *et al.* 2021).

Q. polygnathiformis magna was first established in the Carnian in Japan (Igo, 1989). The reported *Q.* aff. *polygnathiformis magna* in the Yize section is similar to *Q. polygnathiformis magna* in its bifurcated keel end but differs in its platform outline (Igo, 1989). *Q.* aff. *polygnathiformis magna* is regionally common, also known from the Zhuganpo Fm in Yunnan Province (Zhang *et al.* 2018*b*). *Q. wanlanensis* was first established in the Julian in southwestern China (Zhang *et al.* 2017, 2018*b*) and was later also recognized in central Japan (Tomimatsu *et al.* 2021), suggesting the species may be geographically widespread.

4.c. *Quadralella praelindae* Zone

Lower limit: FO of *Q. praelindae.*
Upper limit: FO of *Q. auriformis.*
Associated taxa: *G. malayensis*, *G. tethydis*, *Kraussodontus* (*K.*) *praeangustus*, *P. inclinata*, *Q. acuminata*, *Q. intermedia*, *Q. jiangyouensis*, *Q. lobata*, *Q. polygnathiformis*, *Q.* aff. *polygnathiformis magna*, *Q. shijiangjunensis*, *Q.* spp., *Q. tadpole*, *Q. wanlanensis*, *Q. wayaoensis*, *Q. yongyueensis* and *Q.* aff. *zonneveldi.*

The *Q. praelindae* Zone ranges from the 47.1 m to the 67 m level. *Q. praelindae* was first identified in the lower Tuvalian at Silická Brezová, Slovakia (Kozur, 2003; Channell *et al.* 2003). Later, the species was reported in the Julian strata (Rigo *et al.* 2007; Sun, Z. Y. *et al.* 2016; Zhang *et al.* 2018*b*) (Fig. 7).

The genus *Gladigondolella* has a long range from the Spathian to the end of the Julian. A total of five species, including *G. arcuata*, *G. budurovi*, *G. carinata*, *G. malayensis* and *G. tethydis* are attributed to this genus (Chen *et al.* 2015). *G. tethydis* is known from the Tethys and Panthalassa, ranging from the Aegean to the uppermost Julian (Igo, 1989; Kozur, 1989*a*; Gallet *et al.* 1994; Chen *et al.* 2015; Kiliç *et al.* 2017; Zhang *et al.* 2017). *G. malayensis* is characterized by its broader platform and posteriorly located basal cavity and ranges from the Longobardian to the uppermost Julian (Kozur, 2003; Chen *et al.* 2015). *G. malayensis* and *G. tethydis* have been reported in Guizhou Province of South China, ranging from the Aegean to the Julian (Lehrmann *et al.* 2015; Sun, Y. D. *et al.* 2016; Zhang *et al.* 2017).

Q. zonneveldi was established in the Julian in British Columbia (Orchard, 2007). The reported *Q.* aff. *zonneveldi* shares a similar platform outline with *Q. zonneveldi* but has a sunken carina (Fig. 8).

K. praeangustus is the first reported occurrence in southwestern China. The holotype of *K. praeangustus* was established from Julian strata in Romania, and the species is also known in southern Turkey (Kozur, 1980*a*; Chen & Lukeneder, 2017). Compared to *Q. polygnathiformis*, *K. praeangustus* has a slender platform with one/two side constriction(s) in the posterior platform. *Q. shijiangjunensis* and *Q. wayaoensis* have not yet been reported outside of southwestern China.

4.d. *Quadralella auriformis* Zone

Lower limit: FO of *Q. auriformis.*
Upper limit: FO of *Q. robusta.*
Associated taxa: *K. praeangustus*, *Ma. baloghi*, *P. inclinata*, *Q. intermedia*, *Q. lobata*, *Q. polygnathiformis*, *Q. praelindae*, *Q.* spp., *Q. tadpole* and *Q.* aff. *zonneveldi.*

The *Q. auriformis* Zone ranges from the 67 m to the 72.2 m level. This zone has been established in southwestern China, the Alps and the Himalayas (Gallet *et al.* 1994; Krystyn *et al.* 2004; Sun, 2006; Hornung *et al.* 2007). The zonal species is characterized by its ear-like platform and differs from *Q. tadpole* by its expanded middle platform and shorter length (Kovács, 1977; Mastandrea, 1995; Kiliç *et al.* 2015). It ranges from the lower Julian to the lower Tuvalian and is known in the western Tethys, Japan, the Himalayas, northern Oman and southwestern China (Kovács, 1977; Gallet *et al.* 1994; Mastandrea, 1995; Hornung *et al.* 2007; Rigo *et al.* 2007; Kiliç *et al.* 2015; Zhang *et al.* 2018*b*; Sun *et al.* 2019; Tomimatsu *et al.* 2021). The species could be the direct ancestor of *Ma. baloghi* and *Ma. carnica* (Fig. 9).

Ma. baloghi is reported for the first time here in southwestern China. The species shares many common features with *Q. auriformis* but has distinct nodes on the anterior platform margins (Kovács, 1977; Mastandrea, 1995). It has a short range within the Julian substage and is known in Hungary, Oman and Italy (e.g. Kovács, 1977; Mastandrea, 1995; Rigo *et al.* 2007; Chen *et al.* 2015; Kiliç *et al.* 2015, 2017; Sun *et al.* 2019) (Fig. 10).

https://doi.org/10.1017/S0016756822001236 Published online by Cambridge University Press

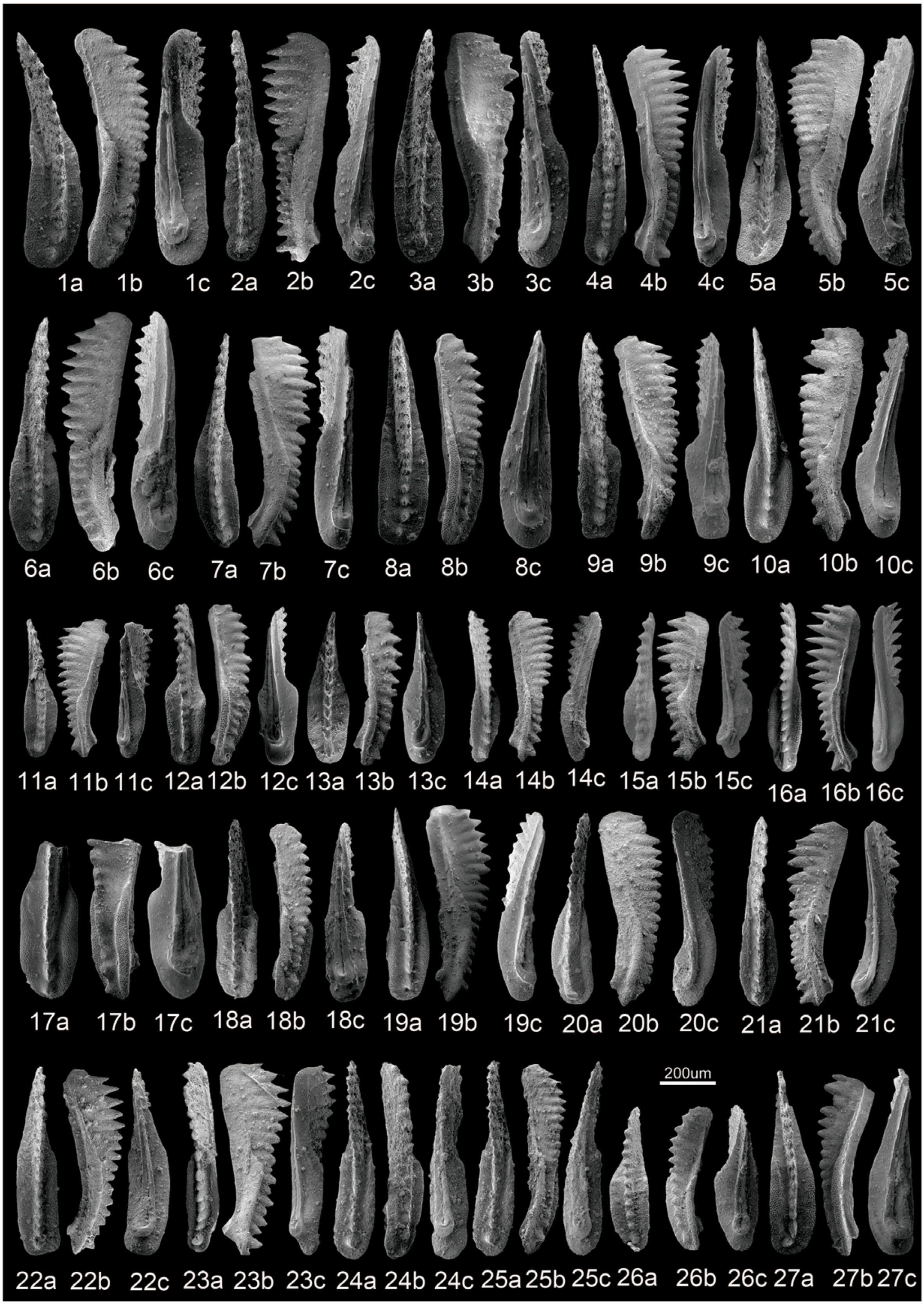

Fig. 5. SEM photographs of conodonts from Ladinian to Carnian strata at Yize. Scale bar = 200 μm. a – upper view; b – lateral view; c – lower view. 1 – *Q. polygnathiformis* (Budurov & Stefanov, 1965), YZ-95-1-029; 2 – *K. praeangustus* (Kozur, Miräuta & Mock *in* Kozur, 1980*b*), YZ-95-1-030; 3 – *Q. jiangyouensis* (Wang & Dai, 1981), YZ-95-1-031; 4 – *K. praeangustus* (Kozur, Miräuta & Mock *in* Kozur, 1980*b*), YZ-95-1-032; 5 – *Q. polygnathiformis* (Budurov & Stefanov, 1965), YZ-95-1-033; 6 – *Q. intermedia* (Orchard, 2007), YZ-95-1-034; 7 – *Q. robusta* Zhang, Sun & Lai *in* Zhang *et al*. 2018*b*, YZ-95-1-036; 8 – *P. inclinata* (Kovács, 1983), YZ-95-1-044; 9 – *Q. jiangyouensis* (Wang & Dai, 1981), YZ-95-1-017; 10 – *Q. tadpole* (Hayashi, 1968), YZ-95-2-046; 11 – *Q. intermedia* (Orchard, 2007), YZ-95-1-061; 12 – *Q.* aff. *zonneveldi* (Orchard, 2007), YZ-95-1-066; 13 – *P. foliata* Budurov, 1975, YZ-95-1-070; 14 – *Q. tadpole* (Hayashi, 1968), YZ-95-2-019; 15 – *Q. praelindae* (Kozur, 2003), YZ-95-1-015; 16 – *Q. praelindae* (Kozur, 2003), YZ-95-1-009; 17 – *Q. intermedia* (Orchard, 2007), YZ-95-2-012; 18 – *Q. polygnathiformis* (Budurov & Stefanov, 1965), YZ-95-2-016; 19 – *Q. polygnathiformis* (Budurov & Stefanov, 1965), YZ-95-2-024; 20 – *Q. robusta* Zhang, Sun & Lai *in* Zhang *et al*. 2018*b*, YZ-95-2-045; 21 – *Q. robusta* Zhang, Sun & Lai *in* Zhang *et al*. 2018*b*, YZ-95-2-047; 22 – *Q. jiangyouensis* (Wang & Dai, 1981), YZ-95-2-049; 23 – *K. praeangustus* (Kozur, Miräuta & Mock *in* Kozur, 1980*b*), YZ-95-2-051; 24 – *K. praeangustus* (Kozur, Miräuta & Mock *in* Kozur, 1980*b*), YZ-95-2-052; 25 – *K. praeangustus* (Kozur, Miräuta & Mock *in* Kozur, 1980*b*), YZ-95-2-053; 26 – *P. inclinata* (Kovács, 1983), YZ-99-025; 27 – *P. inclinata* (Kovács, 1983), YZ-12-2-002.

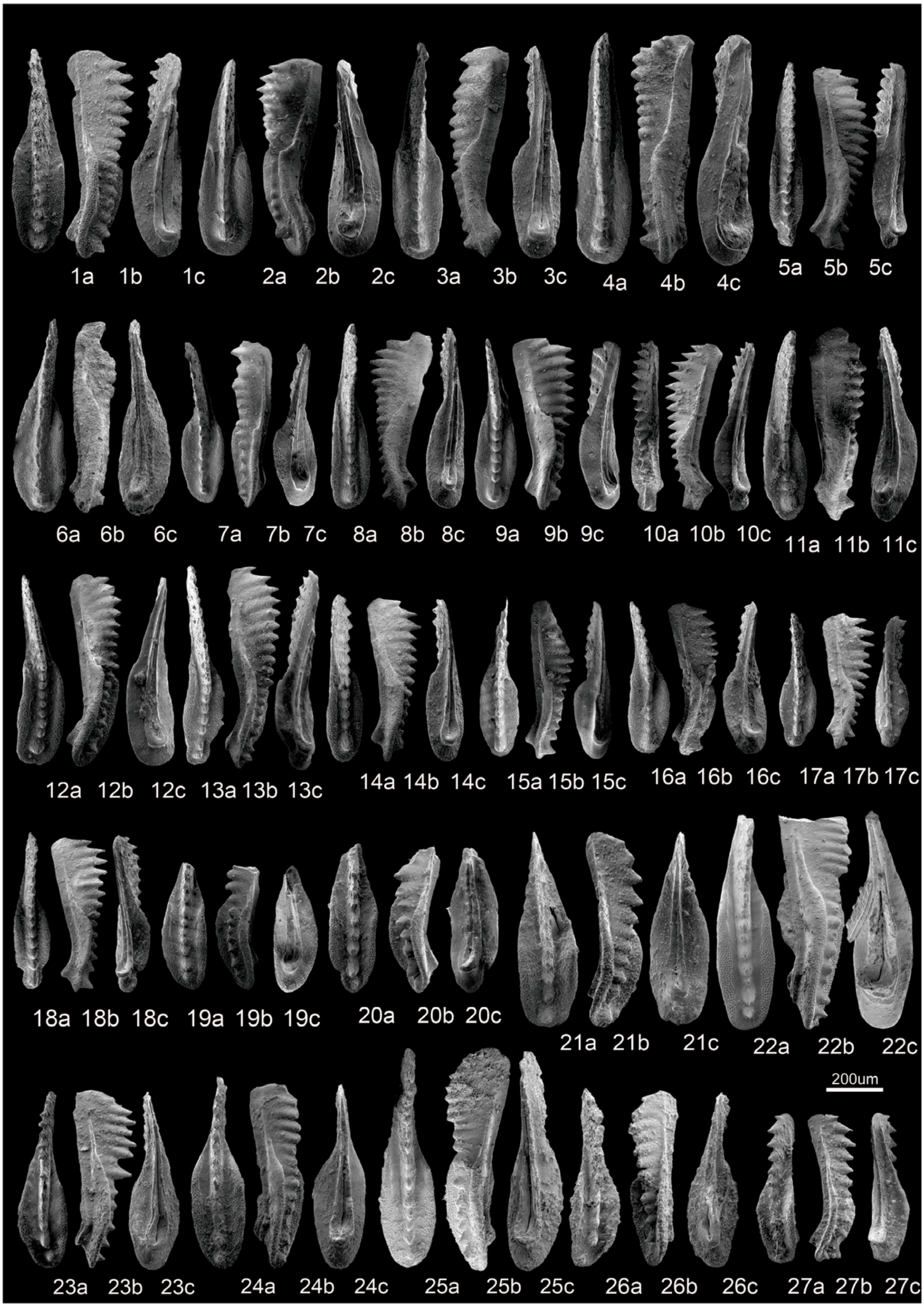

Fig. 6. SEM photographs of conodonts from Ladinian to Carnian strata at Yize. Scale bar = 200 µm. a – upper view; b – lateral view; c – lower view. 1 – *Q. intermedia* (Orchard, 2007), YZ-95-1-004; 2 – *Q. polygnathiformis* (Budurov & Stefanov, 1965), YZ-88-1-17; 3 – *Q. polygnathiformis* (Budurov & Stefanov, 1965), YZ-88-1-18; 4 – *Q. polygnathiformis* (Budurov & Stefanov, 1965), YZ-88-1-19; 5 – *Q. praelindae* (Kozur, 2003), YZ-88-1-08; 6 – *Q. intermedia* (Orchard, 2007), YZ-88-1-01; 7 – *Q. tadpole* (Hayashi, 1968), YZ-88-1-04; 8 – *Q. polygnathiformis* (Budurov & Stefanov, 1965), YZ-88-1-05; 9 – *Q. polygnathiformis* (Budurov & Stefanov, 1965), YZ-88-1-07; 10 – *Q. praelindae* (Kozur, 2003), YZ-88-1-12; 11 – *Q. tadpole* (Hayashi, 1968), YZ-88-1-16; 12 – *Q. polygnathiformis* (Budurov & Stefanov, 1965), YZ-88-1-14; 13 – *Q. praelindae* (Kozur, 2003), YZ-88-2-03; 14 – *Q. polygnathiformis* (Budurov & Stefanov, 1965), YZ-88-1-15; 15 – *Q. intermedia* (Orchard, 2007), YZ-88-2-16; 16 – *Q. intermedia* (Orchard, 2007), YZ-88-2-21; 17 – *Q.* sp., YZ-95-2-057; 18 – *Q. praelindae* (Kozur, 2003), YZ-88-1-09; 19 – *Q. intermedia* (Orchard, 2007), YZ-88-2-22; 20 – *Q. acuminata* (Orchard, 2007), YZ-(-17)2-001; 21 – *P. inclinata* (Kovács, 1983), YZ-(-17)2-002; 22 – *Q. polygnathiformis* (Budurov & Stefanov, 1965), YZ-(-65)-i001; 23 – *Q. acuminata* (Orchard, 2007), YZ-(-65)-004; 24 – *Q. intermedia* (Orchard, 2007), YZ-(-65)-005; 25 – *Q. intermedia* (Orchard, 2007), YZ-(-65)-i005; 26 – *P. foliata* Budurov, 1975, YZ-(-65)-012; 27 – *P. inclinata* (Kovács, 1983), YZ-(-17)2-003.

https://doi.org/10.1017/S0016756822001236 Published online by Cambridge University Press

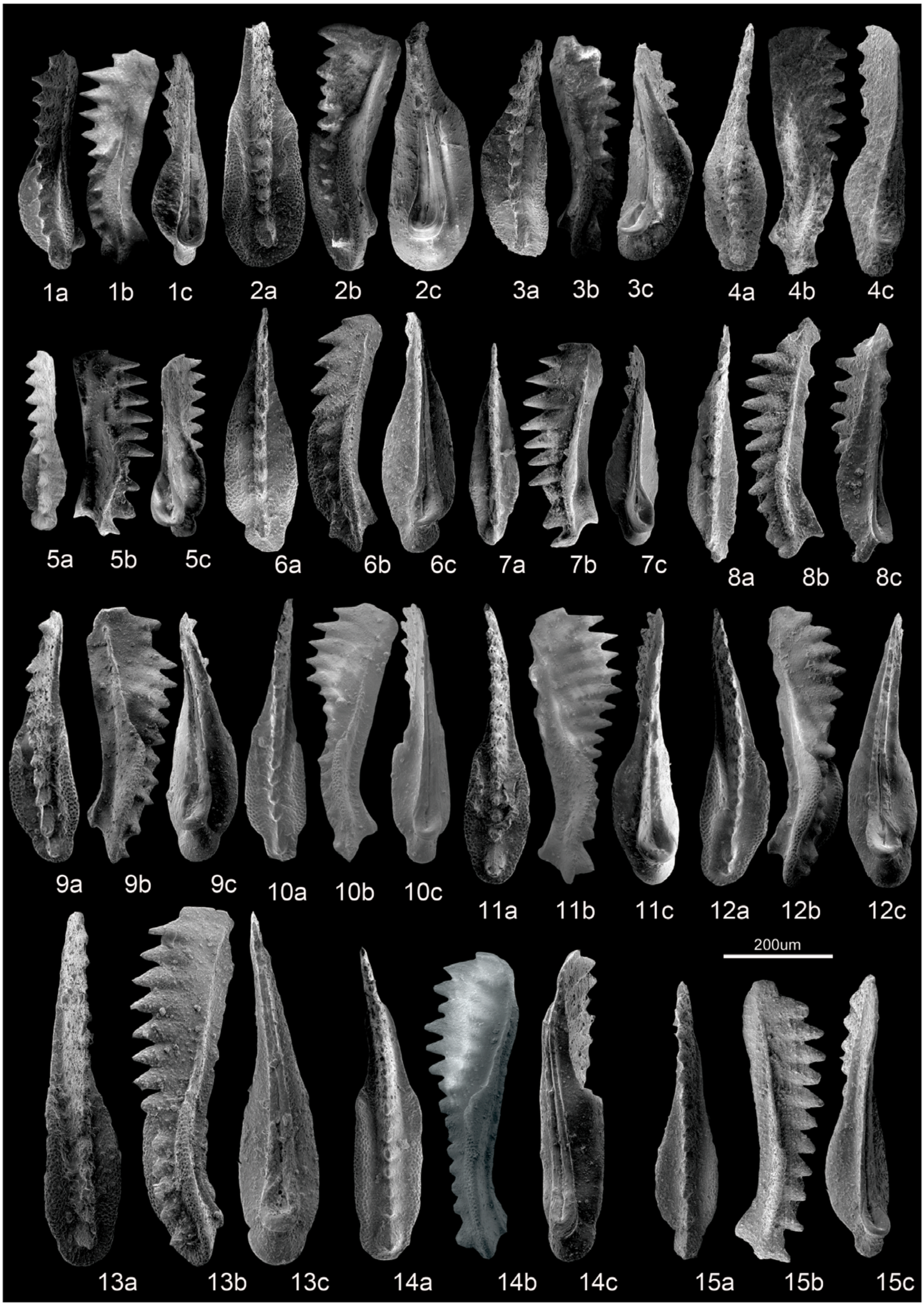

Fig. 7. SEM photographs of conodonts from Ladinian to Carnian strata at Yize. Scale bar = 200 μm. a – upper view; b – for lateral view; c – for lower view. 1 – *Q.* sp., YZ-88-1-50; 2 – *Q. polygnathiformis* (Budurov & Stefanov, 1965), YZ-79-022; 3 – *P. inclinata* (Kovács, 1983), YZ-79-023; 4 – *Q. tadpole* (Hayashi, 1968), YZ-79-003; 5 – *Q.* sp., YZ-46-008; 6 – *Q. lobata* (Orchard, 2007), YZ-12-1-020; 7 – *Q. praelindae* (Kozur, 2003), YZ-74-014; 8 – *Q. praelindae* (Kozur, 2003), YZ-74-015; 9 – *Q. acuminata* (Orchard, 2007), YZ-12-1-001; 10 – *Q. praelindae* (Kozur, 2003), YZ-88-1-58; 11 – *Q. tadpole* (Hayashi, 1968), YZ-88-1-47; 12 – *Q. intermedia* (Orchard, 2007), YZ-88-1-42; 13 – *P. inclinata* (Kovács, 1983), YZ-95-1-020; 14 – *K. praeangustus* (Kozur, Miräuta & Mock *in* Kozur, 1980*b*), YZ-88-1-39; 15 – *Q. praelindae* (Kozur, 2003), YZ-95-1-018.

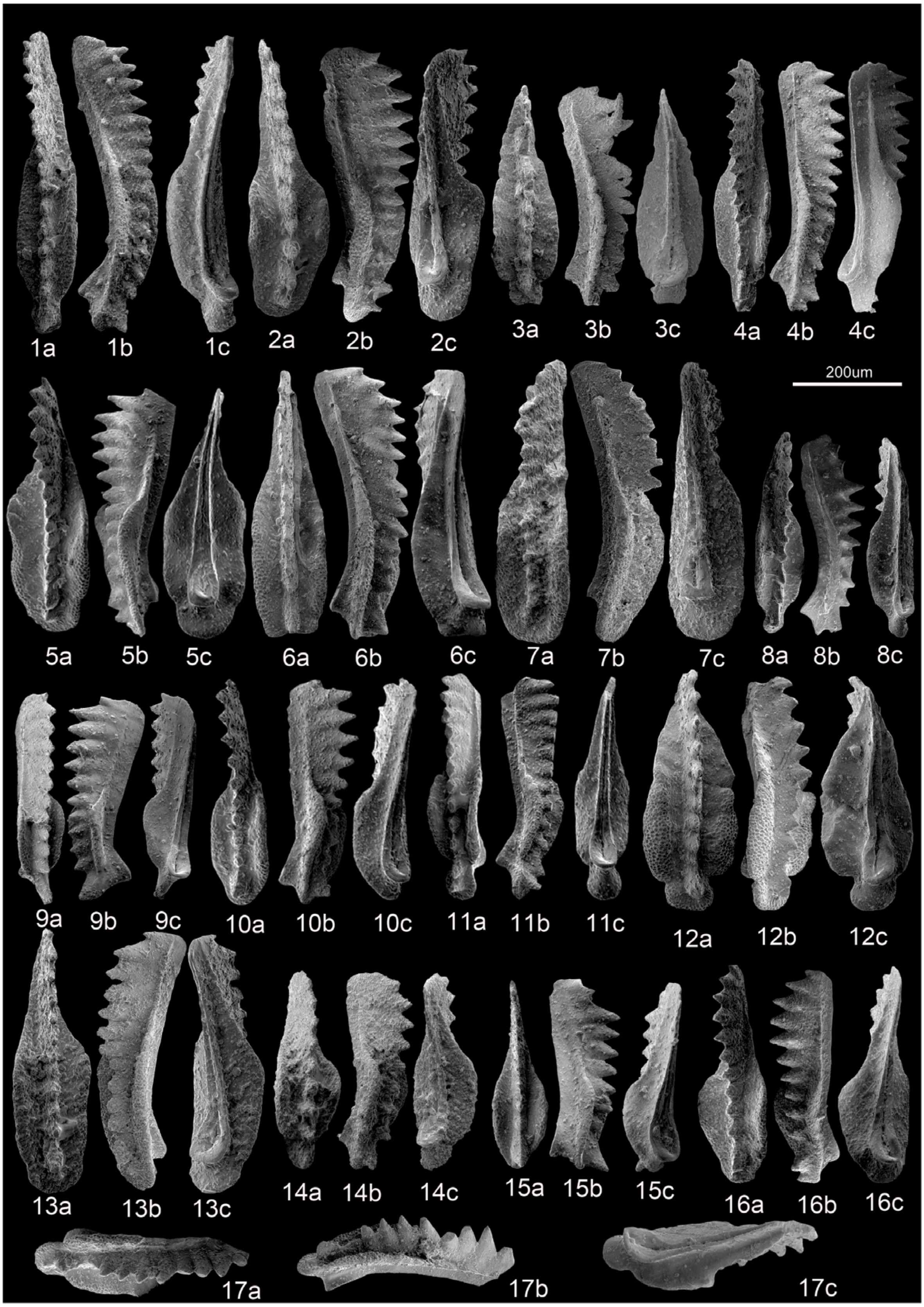

Fig. 8. SEM photographs of conodonts from Ladinian to Carnian strata at Yize. Scale bar = 200 μm. a – upper view; b – lateral view; c – lower view. 1 – *Q. praelindae* (Kozur, 2003), YZ-95-1-025; 2 – *Q.* aff. *zonneveldi* (Orchard, 2007), YZ-95-1-049; 3 – *Q. lobata* (Orchard, 2007), YZ-39-1-038; 4 – *Q. praelindae* (Kozur, 2003), YZ-95-2-032; 5 – *Q. lobata* (Orchard, 2007), YZ-88-1-03; 6 – *P. inclinata* (Kovács, 1983), YZ-15-001; 7 – *Q. polygnathiformis* (Budurov & Stefanov, 1965), YZ-39-1-052; 8 – *Q. praelindae* (Kozur, 2003), YZ-95-2-027; 9 – *Q. auriformis* (Kovács, 1977), YZ-95-2-038; 10 – *Q. tadpole* (Hayashi, 1968), YZ-88-1-06; 11 – *Q. praelindae* (Kozur, 2003), YZ-88-1-24; 12 – *Q. lobata* (Orchard, 2007), YZ-39-1-009; 13 – *P. inclinata* (Kovács, 1983), YZ-39-1-055; 14 – *Q. auriformis* (Kovács, 1977), YZ-99-031; 15 – *Q.* sp., YZ-12-2-022; 16 – *Q. auriformis* (Kovács, 1977), YZ-88-1-33; 17 – *Q. lobata* (Orchard, 2007), YZ-39-1-012.

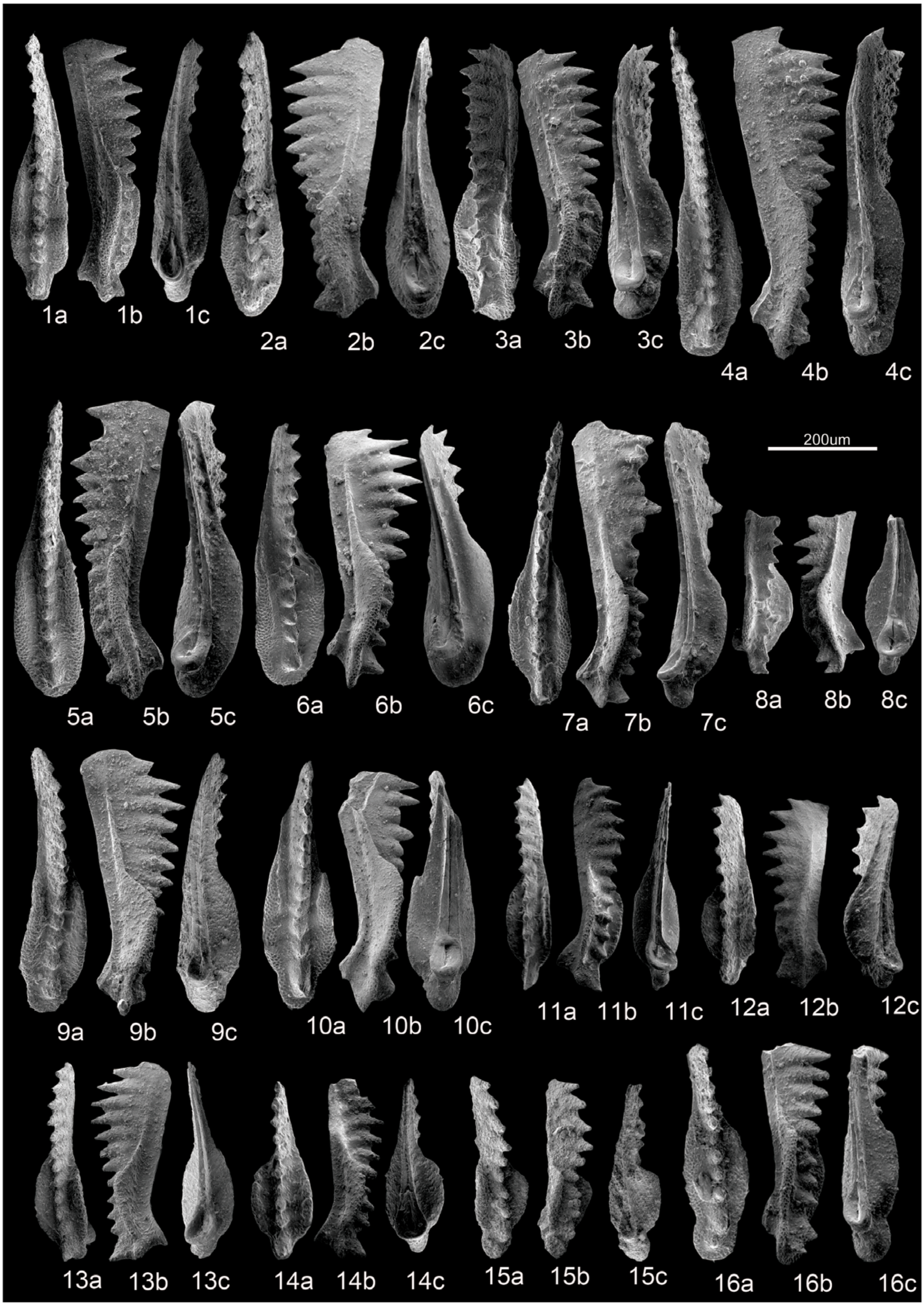

Fig. 9. SEM photographs of conodonts from Ladinian to Carnian strata at Yize. Scale bar = 200 μm. a – upper view; b – lateral view; c – lower view. 1 – *Q. praelindae* (Kozur, 2003), YZ-88-2-04; 2 – *Q. tadpole* (Hayashi, 1968), YZ-88-2-08; 3 – *Q. tadpole* (Hayashi, 1968), YZ-88-2-46; 4 – *K. praeangustus* (Kozur, Mirăuta & Mock *in* Kozur, 1980*b*), YZ-88-2-42; 5 – *Q. intermedia* (Orchard, 2007), YZ-88-2-44; 6 – *Q. polygnathiformis* (Budurov & Stefanov, 1965), YZ-88-3-07; 7 – *Q. praelindae* (Kozur, 2003), YZ-88-3-16; 8 – *Q. auriformis* (Kovács, 1977), YZ-88-3-75; 9 – *Q. praelindae* (Kozur, 2003), YZ-88-3-17; 10 – *Q.* sp., YZ-88-2-38; 11 – *Q. praelindae* (Kozur, 2003), YZ-88-1-64; 12 – *Q.* sp., YZ-88-1-60; 13 – *Q.* sp., YZ-88-2-43; 14 – *Ma. baloghi* (Kovács, 1977), YZ-88-1-63; 15 – *Q. auriformis* (Kovács, 1977), YZ-88-2-26; 16 – *Q.* sp., YZ-88-2-12.

https://doi.org/10.1017/S0016756822001236 Published online by Cambridge University Press

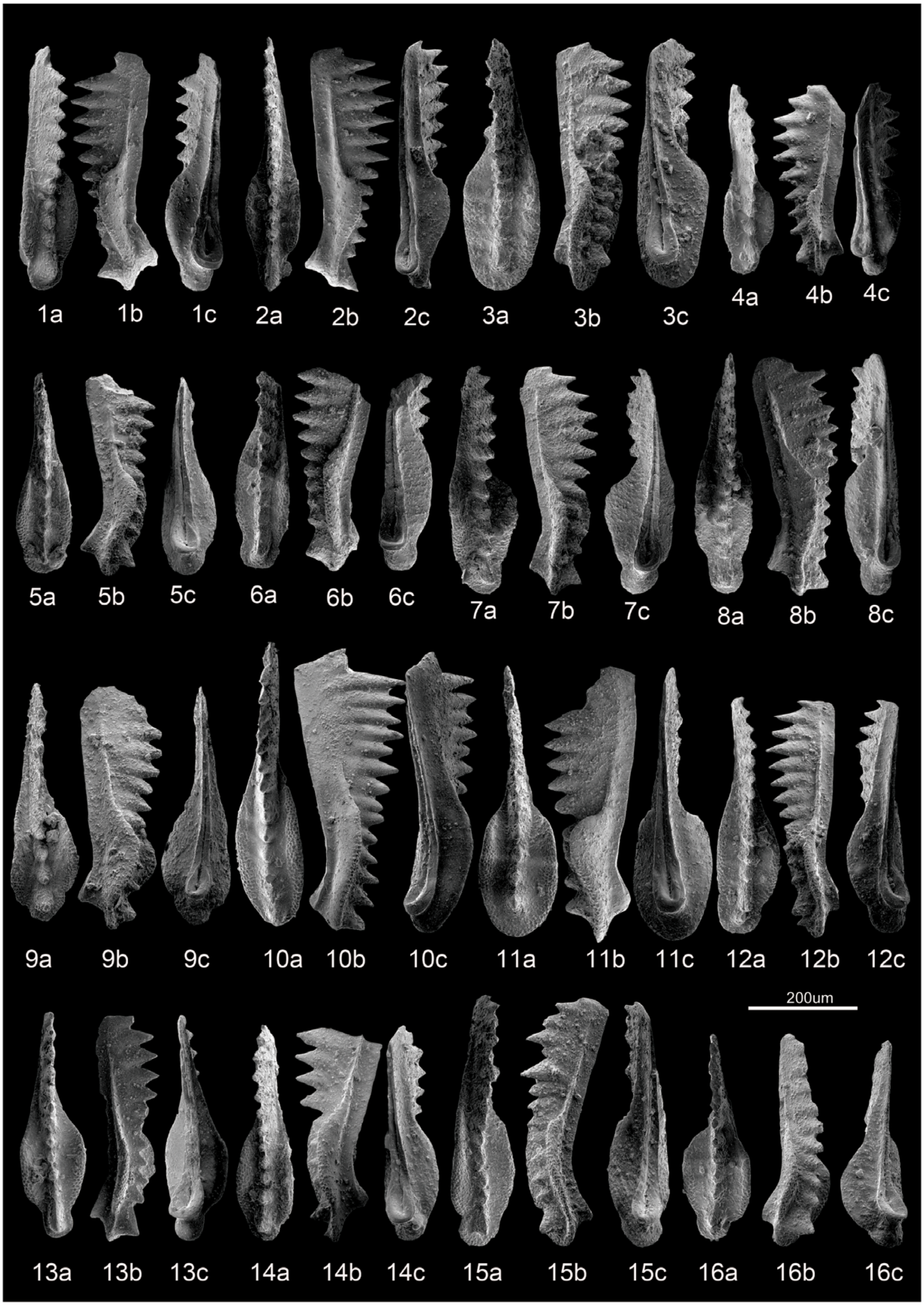

Fig. 10. SEM photographs of conodonts from Ladinian to Carnian strata at Yize. Scale bar = 200 μm. a – upper view; b – lateral view; c – lower view. 1 – *Q. praelindae* (Kozur, 2003), YZ-88-3-24; 2 – *Q. praelindae* (Kozur, 2003), YZ-88-3-38; 3 – *Q. intermedia* (Orchard, 2007), YZ-88-3-32; 4 – *Q.* sp., YZ-88-3-35; 5 – *Q. tadpole* (Hayashi, 1968), YZ-88-3-41; 6 – *Q. praelindae* (Kozur, 2003), YZ-88-3-43; 7 – *Q. auriformis* (Kovács, 1977), YZ-88-3-44; 8 – *Q. praelindae* (Kozur, 2003), YZ-88-3-49; 9 – *Q. auriformis* (Kovács, 1977), YZ-88-3-60; 10 – *Q. tadpole* (Hayashi, 1968), YZ-88-3-61; 11 – *Q. tadpole* (Hayashi, 1968), YZ-88-3-63; 12 – *Q. tadpole* (Hayashi, 1968), YZ-88-3-66; 13 – *Q. auriformis* (Kovács, 1977), YZ-88-2-54; 14 – *Q.* sp., YZ-88-2-63; 15 – *Q. tadpole* (Hayashi, 1968), YZ-88-3-05; 16 – *Q. auriformis* (Kovács, 1977), YZ-88-3-13.

https://doi.org/10.1017/S0016756822001236 Published online by Cambridge University Press

4.e. *Quadralella robusta* Zone

Lower limit: FO of *Q. robusta.*
Upper limit: not defined.
Associated taxa: *K. praeangustus*, *P. foliata*, *P. inclinata*, *Q. acuminata*, *Q. auriformis*, *Q. intermedia*, *Q. jiangyouensis*, *Q. lobata*, *Q. polygnathiformis*, *Q. praelindae*, *Q.* spp., *Q. tadpole* and *Q.* aff. *zonneveldi.*

The *Q. robusta* Zone ranges from the 72.2 m level to the top of the section. This regionally important zone was widely recognized in Julian strata in southwestern China (Zhang *et al.* 2017, 2018*b*). *Q. robusta* is characterized by having a large platform and a robust main cusp (in mature form). The species is common in the Zhuganpo and Wayao boundary beds and ranges from the uppermost Julian 1 to the lowermost Tuvalian 1? (Sun, Y. D. *et al.* 2016; Zhang *et al.* 2017, 2018*b*).

5. Discussion

5.a. Conodont palaeogeography and ecology

Early Carnian conodonts show significant provincialism on the globe (Mosher, 1968; Budurov *et al.* 1985; Lai & Mei, 2000; Klets, 2008; Chen *et al.* 2015; Martínez-Pérez *et al.* 2015; Zhang *et al.* 2018*b*). The genera *Paragondolella*, *Gladigondolella*, *Pseudofurnishius*, *Quadralella*, *Mazzaella* and *Budurovignathus* dominated the Julian assemblages in the western Tethys, while *Mosherella*, *Paragondolella* and *Quadralella* are common in North America. Only a few monotonous *Budurovignathus* and a single *Gladigondolella* species have been reported in North America (e.g. Mosher, 1968; Orchard *et al.* 2001; Balini *et al.* 2007; Orchard & Balini, 2007; Orchard, 2010). *Mosherella* was rare in the western Tethys and only reported in southern Turkey (e.g. Orchard, 2010; Chen & Lukeneder, 2017). In the Panthalassa and the Himalayas, *Paragondolella*, *Quadralella*, *Gladigondolella* and *Budurovignathus* were common in the Julian (e.g. Koike *et al.* 1991; Krystyn *et al.* 2004; Zhang *et al.* 2019).

In South China, conodont assemblages are dominated by genera of *Paragondolella* and *Quadralella* in the Julian, while *Mosherella*, *Pseudofurnishius*, *Gladigondolella* and *Budurovignathus* are very rare (Yang *et al.* 1995, 2002; Wang *et al.* 2005; Dong & Wang, 2006; Sun, 2006; Sun, Y. D. *et al.* 2016; Sun, Z. Y. *et al.* 2016; Zhang *et al.* 2017, 2018*b*). At the species level, indigenous species are more common. However, Julian conodonts from southwestern China still share many common features with those from the western Tethys and North America, laying a biostratigraphic foundation for supra-regional correlation.

Conodont distribution is controlled, in part, by their ecology, i.e. the dwelling habitats of conodont animals (Kozur, 1976; Lai *et al.* 2001; Chen *et al.* 2021). This is more conspicuous in the Middle and Late Triassic amongst the genera *Gladigondolella* and *Budurovignathus*. *Gladigondolella* was considered a pelagic conodont element restricted to the Tethys realm, part of Panthalassa and the western margin of North America (Kozur, 1976; Kozur *et al.* 2009). Two species, namely *G. tethydis* and *G. malayensis*, are most common in the western Tethys and Panthalassa but are rather rare in South China (e.g. Koike *et al.* 1991; Gallet *et al.* 1994; Balini *et al.* 2000; Wang *et al.* 2005; Lein *et al.* 2012; Zhang *et al.* 2017; Tomimatsu *et al.* 2021). They have never occurred in a platform setting, suggesting the taxa may have favoured deeper water habitats (also see Trotter *et al.* 2015).

Abundant and diverse *Budurovignathus* species occur in various environments in the western Tethys (e.g. Gallet *et al.* 1994; Mastandrea *et al.* 1997; Loriga *et al.* 1998; Balini *et al.* 2000; Mietto *et al.* 2007, 2012; Richoz *et al.* 2007; Rigo *et al.* 2007; Lein *et al.* 2012; Stocker *et al.* 2013; Muttoni *et al.* 2014; Karádi *et al.* 2022). Owing to common occurrences of *Budurovignathus* species in European sections, the FAD of *B. diebeli* and the last appearance of *B. mungoensis* were proposed as markers for the L-CB (Kozur & Mostler, 1971; Kozur, 1989*b*). However, these species are rare in other regions, and the FAD of *B. diebeli* was later proved in the Longobardian (e.g. Krystyn, 1983; Loriga *et al.* 1998; Karádi *et al.* 2022). In South China, *Budurovignathus* species are very rare and by far best known from Guandao, which represents an oxygenated platform margin environment (Wang *et al.* 2005; Enos *et al.* 2006; Lehrmann *et al.* 2015). *Budurovignathus* specimens are also reported at Guanyinya in northern Sichuan and Dapingzi in Guizhou (Jiang *et al.* 2018, 2019). However, these elements do not develop nodes on their anterior platform margins or have denticles on the platform and are very unusual. In British Columbia and Nevada, *Budurovignathus* species are found in diverse environments from slope to basin but were never very diverse (Balini & Jenks, 2007; Balini *et al.* 2007; Orchard, 2007, 2010; Orchard & Balini, 2007). In the Indian Himalayas, *Budurovignathus* faunas have been obtained from the Kaga and Chomule formations, which represent a neritic shelf setting below the storm wave base (Bhargava *et al.* 2004; Krystyn *et al.* 2004; Sun *et al.* 2021). Deep-sea sediments in the Panthalassa also contain *Budurovignathus* faunas (Nakada *et al.* 2014; Zhang *et al.* 2019; Tomimatsu *et al.* 2021). These may indicate that *Budurovignathus* could thrive in diverse environments. However, why *Budurovignathus* is so rare in South China remains a mystery.

5.b. The Ladinian–Carnian boundary

Ammonoids and conodonts are favoured as standard biotic indices to define Triassic stage and substage boundaries (Gradstein *et al.* 2020). *Daxatina canadensis* is a popular choice for the base of the Carnian in the western Tethys, North America and Himalayas (e.g. Krystyn *et al.* 2004; Orchard, 2007; Mietto *et al.* 2012). In South China, ammonoid biostratigraphy is not well established for the Upper Triassic. This is mostly attributed to the paucity of ammonoids commonly found in other regions (e.g. Hsu & Chen, 1944; Wang, 1983; Xu *et al.* 2003; Balini *et al.* 2010; Zou *et al.* 2015; Tong *et al.* 2019). Some studies implied that the L-CB should be placed in the upper part of the Zhuganpo Fm or even in the lower Wayao Fm (Xu *et al.* 2003; Li *et al.* 2013; Zou *et al.* 2015).

Conodonts are preferred as important markers to define the L-CB. The FAD of several conodont species, including *B. diebeli*, *Mosherella newpassensis* and *Q. polygnathiformis* have been proposed as auxiliary biotic markers for the L-CB (Mosher, 1968; Kozur & Mostler, 1971; Mietto *et al.* 2007). However, the FAD of *B. diebeli* is lower than the FAD of *Daxatina canadensis*, and *B. diebeli* is not widely distributed (e.g. Krystyn, 1983; Loriga *et al.* 1998; Krystyn *et al.* 2004; Mietto *et al.* 2007, 2012; Orchard, 2010; Plasencia *et al.* 2018; Karádi *et al.* 2022). *Mosherella newpassensis* is known in North America and South China but not in the western Tethys (Orchard, 2010). The FO of *Mosherella newpassensis* also falls in the Longobardian (Wang *et al.* 2005; Lehrmann *et al.* 2015). The FAD of *Q. polygnathiformis* is the most suitable as the practical marker for the L-CB, owing to its global distribution and nearly co-occurrence with *Daxatina canadensis* (Krystyn *et al.* 2004; Sun *et al.* 2005; Rigo *et al.* 2007;

https://doi.org/10.1017/S0016756822001236 Published online by Cambridge University Press

Mietto *et al.* 2007, 2012; Lehrmann *et al.* 2015). However, Orchard (2010) suggested that the occurrence of *Q. polygnathiformis* could be affected by variations in sedimentation rates.

In southwestern China, the position of the L-CB is a matter of debate owing to the difficulties in defining the FO of *Q. polygnathiformis* and a lack of other auxiliary markers. Yang *et al.* (1995) placed the L-CB in the lowermost Zhuganpo Fm based on massive occurrences of *Q. polygnathiformis*. Sun *et al.* (2005) argued that the L-CB should be put at the 3.38 m level in the Zhuganpo Fm based on the evolutionary lineage of *P. inclinata* – *Q. polygnathiformis* – *Q. maantangensis* and the FO of *Q. polygnathiformis*. Zhang *et al.* (2017) suggested that the L-CB is unlikely lower than the lithological boundary between the Yangliujing and Zhuganpo formations. These minor discrepancies could be due to a lack of robust biostratigraphic control in the L-CB beds and might also point to the diachronous nature of the Zhuganpo Fm.

The *Q. intermedia* Zone has been proposed as the first Carnian conodont zone in British Columbia. The FO of *Q. intermedia* is a practical auxiliary biotic marker for the L-CB because it co-occurred with *Daxatina canadensis* in the *Frankites sutherlandi* Zone (Balini *et al.* 2007; Orchard, 2007, 2010; Chen *et al.* 2015). At Yize, the FOs of *Q. polygnathiformis* and *Q. intermedia* occur at the same level, suggesting that the L-CB should be placed in the lower cherty limestone member. However, age-diagnostic conodonts are lacking from the 14 m to the 29 m level at the transition from the fine-laminated member to the cherty limestone member. It is possible that the FAD of *polygnathiformis* and *intermedia*, i.e. the true L-CB, is within this interval.

5.c. Strata correlation using conodont zonation

Short-ranged and widely distributed conodont taxa have been favoured as zonal species. At Yize, the *P. inclinata* Zone is likely the last Ladinian zone or straddles the L-CB, as the species is known worldwide in various environments (e.g. Kovács, 1983; Orchard, 2007; Rigo *et al.* 2007; Lein *et al.* 2012; Lehrmann *et al.* 2015; Tomimatsu *et al.* 2021). The established *Q. polygnathiformis* Zone at Yize could correlate to the *Q. intermedia* Zone in British Columbia and Nevada and the *Q. polygnathiformis* IZ in the western Tethys and Panthalassa Ocean (Koike, 1979; Orchard, 2007, 2010; Rigo *et al.* 2018). The *Q. auriformis* Zone is an important zone that is well correlated to the western Tethys, the Indian Himalayas and the Panthalassa due to its clear evolutionary lineage, widespreadness and short range (e.g. Gallet *et al.* 1994; Hornung *et al.* 2007; Tomimatsu *et al.* 2021). The *Q. robusta* Zone could be a practical zone for regional correlation in southwestern China. This zone is immediately below the *Ma. carnica* Zone and correlates well with the widespread Carnian Humid Episode in the Julian 1 to Julian 2 transition (Hornung *et al.* 2007; Zhang *et al.* 2018*a*,*b*).

5.d. Implications for conodont evolution

Conodonts were reasonably diverse in much of the Late Triassic period and show tendencies toward (i) shortening of the platform, (ii) increasing ornaments on the platform and (iii) forward-shifting of the basal cavity (Mazza *et al.* 2010, 2012; Kiliç *et al.* 2015; Karádi, 2021).

Shortening of the platform is a general trend that has been observed amongst gondolellids since the late Middle Triassic period. Two lineages, *P. excelsa* – *P. inclinata* – *P. foliata* – *Q. tadpole* and *Q. acuminata* – *Q. intermedia*, were recognized by a decreasing anterior platform from the Longobardian to the Julian in Hungary and British Columbia (Kovács, 1983; Orchard, 2007; Orchard & Balini, 2007). Such changes were later widely recognized in the western Tethys and southwestern China (Sun *et al.* 2005; Kiliç *et al.* 2015, 2017; Zhang *et al.* 2017, 2018*b*).

The ornamented anterior platform is a most distinctive feature amongst gondolellids in the late Longobardian to the Julian. A transition from smooth to nodose or denticulated platforms is first seen in the *B. japonica* – *B. mungoensis* – *B. diebeli* lineage and in *B. mostleri* (e.g. Balini *et al.* 2000; Chen *et al.* 2015; Plasencia *et al.* 2018). This evolutionary trend is not yet seen in South China and North America owing to the paucity of *Budurovignathus* elements. However, a similar evolutionary trend is seen in the *Q. auriformis* – *Ma. baloghi* – *Ma. carnica* lineage in the Julian substage (Kovács, 1977; Mastandrea, 1995; Kiliç *et al.* 2015; Sun *et al.* 2019).

The forward-shifting pit was typically seen amongst late Tuvalian conodonts, especially in *Metapolygnathus* and *Carnepigondolella* (e.g. Mazza *et al.* 2010; Kiliç *et al.* 2017). However, in southwestern China, this change seems to occur earlier in the Julian, evidenced by the appearances of *Q. langdaiensis*, *Q. maantangensis*, *Q. wanlanensis* and *Q. polygnathiformis magna*, which all have obviously forward-shifted pits (Zhang *et al.* 2017).

6. Conclusions

Conodont taxonomy and biostratigraphy were investigated in detail at Yize, Yunnan, southwestern China. The Yize conodont fauna represents a typical late Ladinian to early Carnian assemblage with both endemic and cosmopolitan forms. The FOs of *Q. polygnathiformis* and *Q. intermedia* are practical markers co-defining the L-CB in the cherty limestone member of the Zhuganpo Fm. Five conodont zones, namely, the *P. inclinata* Zone, the *Q. polygnathiformis* Zone, the *Q. praelindae* Zone, the *Q. auriformis* Zone and the *Q. robusta* Zone, are established and represent a practical biostratigraphic framework in the region. The Zhuganpo Fm, one of the most essential Upper Triassic units in South China, could be diachronous and brackets at least the uppermost Ladinian to the lower Carnian.

Acknowledgements. This study is financially supported by the Natural Science Foundation of China [grant No. 41830320, 41821001 and 42272022], State Key Laboratory of Palaeobiology and Stratigraphy (Nanjing Institute of Geology and Palaeontology, CAS) [grant No. 203123] and China Geological Survey [grant No. DD20211391]. Reviewers Viktor Karádi and Yixing Du are thanked for their constructive comments. G. Q. Liu (Nanchang), Q. Wu (Nanjing), J. Chen (Qingdao), Y. Z. Huang (Nanjing), L. N. Wang (Shijiazhuang), X. L. Wu (Wuhan) and J. L. Fu (Wuhan) are thanked for field and lab assistance.

Conflict of interest. None.

References

Balini M, Germani D, Nicora A and Rizzi E (2000) Ladinian/Carnian ammonoids and conodonts from the classic Schilpario-Pizzo Camino area (Lombardy): revaluation of the biostratigraphic support to chronostratigraphy and paleogeography. *Rivista Italiana di Paleontologia e Stratigrafia* **106**, 19–58.

Balini M and Jenks JF (2007) The Trachyceratidae from South Canyon (Central Nevada): record, taxonomic problems and stratigraphic significance for the definition of the Ladinian-Carnian boundary. In *The Global Triassic* (eds SG Lucas and JA Spielmann), pp. 14–22. New Mexico Museum of Natural History and Science Bulletin 41.

Balini M, Jenks JF, McRoberts CA and Orchard MJ (2007) The Ladinian-Carnian boundary succession at South Canyon (New Pass Range, Central

Nevada). In *Triassic of the American West* (eds SG Lucas and JA Spielmann), pp. 127–38. New Mexico Museum of Natural History and Science Bulletin 40.
Balini M, Lucas SG, Jenks JF and Spielmann JA (2010) Triassic ammonoid biostratigraphy: an overview. In *The Triassic Timescale* (ed. SG Lucas), pp. 221–62. Geological Society of London, Special Publication no. 334.
Benton MJ, Forth J and Langer MC (2014) Models for the rise of the dinosaurs. *Current Biology* **24**, R87–R95.
Benton MJ, Zhang Q, Hu S, Chen Z-Q, Wen W, Liu J, Huang J, Zhou C, Xie T and Tong J (2013) Exceptional vertebrate biotas from the Triassic of China, and the expansion of marine ecosystems after the Permo-Triassic mass extinction. *Earth-Science Reviews* **125**, 199–243.
Bhargava ON, Krystyn L, Balini M, Lein R and Nicora A (2004) Revised litho- and sequence stratigraphy of the Spiti Triassic. *Albertiana* **30**, 21–39.
Budurov K (1975) *Paragondoella foliata* sp. n (Conodonta) von der Trias des Ost-Balkans. *Review of the Bulgarian Geological Society* **36**, 79–81.
Budurov KJ, Gupta V, Sudar MN and Buryi GJ (1985) Conodont zonation, biofacies and provinces in the Triassic. *Geological Society of India* **26**, 84–94.
Budurov K and Stefanov S (1965) Gattung Gondolella aus der Trias Bulgariens. *Doklady Bolgarskoy Akademiya Nauk, Série Paléontologie* **7**, 115–27.
Budurov KJ and Sudar MN (1990) Late Triassic conodont stratigraphy. *Courier Forschungsinstitut Senckenberg* **118**, 203–39.
Channell JET, Kozur HW, Sievers T, Mock R, Aubrecht R and Sykora M (2003) Carnian–Norian biomagnetostratigraphy at Silická Brezová (Slovakia): correlation to other Tethyan sections and to the Newark Basin. *Palaeogeography, Palaeoclimatology, Palaeoecology* **191**, 65–109.
Chen Z-Q and Benton MJ (2012) The timing and pattern of biotic recovery following the end-Permian mass extinction. *Nature Geoscience* **5**, 375–83.
Chen YL, Joachimski MM, Richoz S, Krystyn L, Aljinović D, Smirčić D, Kolar-Jurkovšek T, Lai XL and Zhang ZF (2021) Smithian and Spathian (Early Triassic) conodonts from Oman and Croatia and their depth habitat revealed. *Global and Planetary Change* **196**, 103362. doi: 10.1016/j.gloplacha.2020.103362.
Chen YL, Krystyn L, Orchard MJ, Lai XL and Richoz S (2015) A review of the evolution, biostratigraphy, provincialism and diversity of Middle and early Late Triassic conodonts. *Papers in Palaeontology* **2**, 235–63.
Chen YL and Lukeneder A (2017) Late Triassic (Julian) conodont biostratigraphy of a transition from reefal limestones to deep-water environments on the Cimmerian terranes (Taurus Mountains, southern Turkey). *Papers in Palaeontology* **3**, 441–60.
Dong ZZ and Wang W (2006) *The Cambrian-Triassic Conodont Faunas in Yunnan, China—Correlative Biostratigraphy and the Study of Palaeobiogeographic Province of Conodont*. Kunming: Yunnan Science and Technology Press (in Chinese with English summary).
Enos P, Lehrmann DJ, Wei JY, Yu YY, Xiao JF, Chaikin DH, Minzoni M, Berry AK and Montgomery P (2006) *Triassic Evolution of the Yangtze Platform in Guizhou Province, People's Republic of China*. Geological Society of America, Special Papers vol. 417, 105 pp.
Gallet Y, Besse J, Krystyn L, Théveniaut H and Marcoux J (1994) Magnetostratigraphy of the Mayerling section (Austria) and Erenkolu Mezarlik (Turkey) section: improvement of the Carnian (Late Triassic) magnetic polarity time scale. *Earth and Planetary Science Letters* **125**, 173–91.
Gallet Y, Krystyn L and Besse J (1998) Upper Anisian to Lower Carnian magnetostratigraphy from the northern calcareous Alps (Austria). *Journal of Geophysical Research: Solid Earth* **103**, 605–21.
Gradstein F, Ogg J, Schmitz M and Ogg G (2020) *The Geologic Time Scale 2020*. New York: Elsevier.
Harper EM, Forsythe GT and Palmer T (1998) Taphonomy and the Mesozoic Marine revolution: preservation state masks the importance of boring predators. *Palaios* **13**, 352–60.
Hayashi S (1968). The Permian conodonts in chert of the Adoyama Formation, Ashio Mountains, central Japan. *Earth Science* **22**, 63–77.
Hornung T, Brandner R, Krystyn L, Joachimski MM and Keim L (2007) Multistratigraphic constraints on the NW Tethyan "Carnian crisis". In *The Global Triassic* (eds SG Lucas and JA Spielmann), pp. 59–67. New Mexico Museum of Natural History and Science Bulletin 41.
Hsu DY and Chen K (1944) Triassic of southwestern Guizhou. *Geological Review* **9**, 13–33.
Igo H (1989) Mixed conodont elements from Hachiman Town, Mino terrane, central Japan. *Nihon Koseibutsu Gakkai hokoku, kiji* **1989** (156), 270–85.
Jiang HS, Chen Y and Liu F (2018) Research prospects on marine Ladinian-Carnian boundary in Guizhou province. *Earth Science* **43**, 3947–54.
Jiang HS, Yuan JL, Chen Y, Ogg JG and Yan JX (2019) Synchronous onset of the mid-Carnian Pluvial Episode in the East and West Tethys: conodont evidence from Hanwang, Sichuan, South China. *Palaeogeography, Palaeoclimatology, Palaeoecology* **520**, 173–80.
Jin X, Shi ZQ, Rigo M, Franceschi M and Preto N (2018) Carbonate platform crisis in the Carnian (Late Triassic) of Hanwang (Sichuan Basin, South China): insights from conodonts and stable isotope data. *Journal of Asian Earth Sciences* **164**, 104–24.
Karádi V (2021) Evolutionary trends of the genus *Ancyrogondolella* (Conodonta) and related taxa in the Norian (Late Triassic). *Journal of Earth Science* **32**, 700–8.
Karádi V, Budai T, Haas J, Voros A, Piros O, Dunkl I and Toth E (2022) Change from shallow to deep-water environment on an isolated carbonate platform in the Middle Triassic of the Transdanubian Range (Hungary). *Palaeogeography, Palaeoclimatology, Palaeoecology* **587**, 110793. doi: 10.1016/j.palaeo.2021.110793.
Kelley NP and Pyenson ND (2015) Evolutionary innovation and ecology in marine tetrapods from the Triassic to the Anthropocene. *Science* **348**, aaa3716. doi: 10.1126/science.aaa371.
Kiliç AM, Plasencia P, Guex J and Hirsch F (2017) Chapter seven – challenging Darwin: evolution of Triassic conodonts and their struggle for life in a changing world. In *Stratigraphy & Timescales, Volume 2* (ed. M Montenari), pp. 333–89. Cambridge MA: Academic Press.
Kiliç AM, Plasencia P, Ishida K and Hirsch F (2015) The case of the Carnian (Triassic) conodont genus *Metapolygnathus* Hayashi. *Journal of Earth Science* **26**, 219–23.
Koike T (1979) Biostratigraphy of Triassic conodonts. In *Biostratigraphy of Permian and Triassic Conodonts and Holothurian Sclerites in Japan* (eds T Koike and H Igo), pp. 21–77. Tokyo: Commemorative Volume of the Retirement of Professor Mosaburo Kanuma (in Japanese).
Koike T (1982) Review of some platform conodonts of the Middle and Late Triassic in Japan. *Science Reports of the Yokohama National University, Section II* **29**, 15–27.
Koike T, Kodachi Y, Matsuno T and Baba H (1991) Triassic conodonts from exotic blocks of limestone in northern Kuzuu, the Ashio Mountains. *Science Reports of the Yokohama National University Section II* **38**, 53–69.
Kovács S (1977) New conodonts from the North Hungarian Triassic. *Acta Mineralogica Petrographica* **23**, 77–90.
Kovács S (1983) On the evolution of excelsa-stock in the Upper Ladinian-Carnian (Conodonta, genus *Gondolella*, Triassic). *Schriftenreihe der Erdwissenschaftlichen Kommissionen* **5**, 107–20.
Kozur HW (1976) Paleoecology of Triassic conodonts and its bearing on multi-element taxonomy. In *Conodont Paleoecology* (ed. CR Barnes), pp. 313–23. The Geological Association of Canada, Special Paper no. 15.
Kozur HW (1980a) Stratigraphische Reichweite der Wichtigsten Conodonten (ohne Zahnreihenconodonten) der Mittel-und Obertrias. *Geologisch-Paläontologische Mitteilungen Innsbruck* **10**,47–78.
Kozur HW (1980b) Revision der conodontenzoierung der Mittel- und Obertrias des tethyalen Faunenreichs. *Geologisch-Paläontologische Mitteilungen Innsbruck* **10**, 79–172.
Kozur HW (1989a) Significance of events in conodont evolution for the Permian and Triassic stratigraphy. *Courier Forschungsinstitut Senckenberg* **117**, 385–408.
Kozur HW (1989b) The taxonomy of the gondolellid conodonts in the Permian and Triassic. *Courier Forschungsinstitut Senckenberg* **117**, 409–69.
Kozur HW (2003) Integrated ammonoid, conodont and radiolarian zonation of the Triassic and some remarks to stage/substage subdivision and the numeric age of the Triassic stages. *Albertiana* **28**, 57–74.
Kozur HW, Moix P and Ozsvart P (2009) New *Spumellaria* (Radiolaria) from the early Tuvalian *Spongotortilispinus moixi* Zone of southeastern Turkey, with some remarks on the age of this fauna. *Jahrbuch der Geologischen Bundesanstalt* **149**, 25–59.
Kozur HW and Mostler H (1971) Probleme der Conodontenforschung in der Trias. *Geologisch-Paläontologische Mitteilungen Innsbruck* **1**, 1–19.

Krystyn L (1980) Triassic conodont localities of the Salzkammergut region. *Abhandlungen der Geologischen Bundesanstalt* **35**, 61–98.

Krystyn L (1983) Das Epidaurus-Profil (Griechenland) – ein Beitrag zur Conodonten-Standardzonierung des tethyalen Ladin und Unterkarn. In *Neue Beiträge zur Biostratigraphie der Tethys-Trias. Schriftenreihe der Erdwissenschaftlichen Kommissionen Österreichische Akademie der Wissenschaften 5* (ed. H Zapfe), pp. 231–58. Vienna: Springer-Verlag.

Krystyn L, Balini M and Nicora A (2004) Lower and Middle Triassic stage and substage boundaries in Spiti. *Albertiana* **30**, 40–53.

Lai XL and Mei SL (2000) On zonation and evolution of Permian and Triassic conodonts. *Developments in Palaeontology and Stratigraphy* **18**, 371–92.

Lai XL, Wignall PB and Zhang KX (2001) Palaeoecology of the conodonts *Hindeodus* and *Clarkina* during the Permian-Triassic transitional period. *Palaeogeography, Palaeoclimatology, Palaeoecology* **171**, 63–72.

Lehrmann DJ, Stepchinski L, Altiner D, Orchard MJ, Montgomery P, Enos P, Ellwood BB, Bowring SA, Ramezani J and Wang H (2015) An integrated biostratigraphy (conodonts and foraminifers) and chronostratigraphy (paleomagnetic reversals, magnetic susceptibility, elemental chemistry, carbon isotopes and geochronology) for the Permian–Upper Triassic strata of Guandao section, Nanpanjiang Basin, South China. *Journal of Asian Earth Sciences* **108**, 117–35.

Lein R, Krystyn L, Sylvain R and Henry L (2012) Middle Triassic platform/basin transition along the Alpine passive continental margin facing the Tethys Ocean – the Gamsstein: the rise and fall of a Wetterstein Limestone Platform (Styria, Austria). *Journal of Alpine Geology* **54**, 471–98.

Li Y, Sun YL, Jiang DY and Hao WC (2013) Carnian (Late Triassic) ammonoid biostratigraphy in Luoping County, Eastern Yunnan Province, China. *Acta Scientiarum Naturalium Universitatis Pekinensis* **49**, 471–9.

Loriga CB, Cirilli S, Zanche VD, Bari DD, Gianolla P, Laghi GF, Lowrie W, Manfrin S, Mastandrea A, Mietto P, Muttoni G, Neri C, Posenato R, Rechichi M, Rettori R and Roghi G (1998) A GSSP candidate for the Ladinian/Carnian boundary, the Prati di Stuores, Stuore, Wiesen section (Dolomites, Italy). *Albertiana* **21**, 2–18.

Klets TV (2008) Paleogeographic regionalisation of Triassic seas based on conodontophorids. *Stratigraphy and Geological Correlation* **16**, 467–89.

Marshall M (2019) A million years of Triassic rain. *Nature* **576**, 26–8.

Martínez-Pérez C, Cascales-Miñana B, Plasencia P and Botella H (2015) Exploring the major depletions of conodont diversity during the Triassic. *Historical Biology* **27**, 503–7.

Mastandrea A (1995) Carnian conodonts from Upper Triassic strata of Tamarin section (San Cassiano Fm., Dolomites, Italy). *Rivista Italiana di Paleontologia e Stratigrafia* **100**, 493–510.

Mastandrea A, Neri C and Russo F (1997) Conodont biostratigraphy of the S Cassiano formation surrounding the Sella Massif (Dolomites, Italy): implications for sequence stratigraphic models of the Triassic of the Southern Alps. *Rivista Italiana di Paleontologia e Stratigrafia* **103**, 39–52.

Mazza M, Cau A and Rigo M (2012) Application of numerical cladistic analyses to the Carnian–Norian conodonts: a new approach for phylogenetic interpretations. *Journal of Systematic Palaeontology* **10**, 401–22.

Mazza M, Furin S, Spötl C and Rigo M (2010) Generic turnovers of Carnian/Norian conodonts: climatic control or competition? *Palaeogeography, Palaeoclimatology, Palaeoecology* **290**, 120–37.

Mietto P, Andreetta R, Broglio LC, Buratti N, Cirilli S, De Zanche V, Furin S, Gianolla P, Manfrin S, Muttoni G, Neri C, Nicora A, Posenato R, Preto N, Rigo M, Roghi G and Spötl C (2007) A candidate of the Global Boundary Stratotype Section and Point for the base of the Carnian Stage (Upper Triassic): GSSP at the base of the *canadensis* Subzone (FAD of *Daxatina*) in the Prati di Stuores/Stuores Wiesen section (Southern Alps, NE Italy). *Albertiana* **36**, 78–97.

Mietto P and Manfrin S (1995) A high resolution Middle Triassic ammonoid standard scale in the Tethys Realm; a preliminary report. *Bulletin de la Société géologique de France* **166**, 539–63.

Mietto P, Manfrin S, Preto N, Rigo M, Roghi G, Furin S, Gianolla P, Posenato R, Muttoni G and Nicora A (2012) The global boundary stratotype section and point (GSSP) of the Carnian stage (Late Triassic) at Prati di Stuores/Stuores Wiesen section (Southern Alps, NE Italy). *Episodes* **35**, 414–30.

Mosher LC (1968) Triassic conodonts from western North America and Europe and their correlation. *Journal of Paleontology* **42**, 895–946.

Mundil R, Palfy J, Renne PR and Brack P (2010) The Triassic timescale: new constraints and a review of geochronological data. In *The Triassic Timescale* (ed. SG Lucas), pp. 41–60. Geological Society of London, Special Publication no. 334.

Mutti M and Weissert H (1995) Triassic monsoonal climate and its signature in Ladinian-Carnian carbonate platforms (Southern Alps, Italy). *Journal of Sedimentary Research* **65**, 357–67.

Muttoni G, Mazza M, Mosher D, Katz ME, Kent DV and Balini M (2014) A Middle–Late Triassic (Ladinian–Rhaetian) carbon and oxygen isotope record from the Tethyan Ocean. *Palaeogeography, Palaeoclimatology, Palaeoecology* **399**, 246–59.

Nakada R, Ogawa K, Suzuki N, Takahashi S and Takahashi Y (2014) Late Triassic compositional changes of aeolian dusts in the pelagic Panthalassa: response to the continental climatic change. *Palaeogeography, Palaeoclimatology, Palaeoecology* **393**, 61–75.

Orchard MJ (2007) New conodonts and zonation, Ladinian-Carnian boundary beds, British Columbia, Canada. In *The Global Triassic* (eds SG Lucas and JA Spielmann), pp. 321–30. New Mexico Museum of Natural History and Science Bulletin 41.

Orchard MJ (2010) Triassic conodonts and their role in stage boundary definition. *The Triassic Timescale* (ed. SG Lucas), pp. 139–61. Geological Society of London, Special Publication no. 334.

Orchard MJ (2013) Five new genera of conodonts from the Carnian-Norian boundary beds of Black Bear Ridge, northeast British Columbia, Canada. In *The Triassic System: New Developments in Stratigraphy and Paleontology* (eds LH Tanner, JA Spielmann and SG Lucas), pp. 445–37. New Mexico Museum of Natural History and Science Bulletin 61.

Orchard MJ and Balini M (2007) Conodonts from the Ladinian-Carnian boundary beds of South Canyon, New Pass Range, Nevada, USA. In *The Global Triassic* (eds SG Lucas and JA Spielmann), pp. 333–40. New Mexico Museum of Natural History and Science Bulletin 41.

Orchard MJ, Cordey F, Rui L, Bamber E, Mamet B, Struik LC, Sano H and Taylor H (2001) Biostratigraphic and biogeographic constraints on the Carboniferous to Jurassic Cache Creek Terrane in central British Columbia. *Canadian Journal of Earth Sciences* **38**, 551–78.

Orchard MJ and Tozer ET (1997) Triassic conodont biochronology, its calibration with the ammonoid standard, and a biostratigraphic summary for the Western Canada Sedimentary Basin. *Bulletin of Canadian Petroleum Geology* **45**, 675–92.

Plasencia P, Kiliç AM, Baud A, Sudar M and Hirsch F (2018) The evolutionary trend of platform denticulation in Middle Triassic acuminate Gondolellidae (Conodonta). *Turkish Journal of Zoology* **42**, 187–97.

Richoz S, Krystyn L and Spötl C (2007) First detailed carbon isotope curve through the Ladinian-Carnian boundary: the Weissenbach section (Austria). *Albertiana* **36**, 98–101.

Rigo M, Mazza M, Karádi V and Nicora A (2018) New Upper Triassic conodont biozonation of the Tethyan Realm. In *The Late Triassic World* (ed. LH Tanner), pp. 189–235. Topics in Geobiology vol. 46. Cham: Springer.

Rigo M, Preto N, Roghi G, Tateo F and Mietto P (2007) A rise in the carbonate compensation depth of western Tethys in the Carnian (Late Triassic): deep-water evidence for the Carnian Pluvial Event. *Palaeogeography, Palaeoclimatology, Palaeoecology* **246**, 188–205.

Shen SZ and Zhang H (2017) What caused the five mass extinctions? *Chinese Science Bulletin* **62**, 1119–35.

Stefani M, Furin S and Gianolla P (2010) The changing climate framework and depositional dynamics of Triassic carbonate platforms from the Dolomites. *Palaeogeography, Palaeoclimatology, Palaeoecology* **290**, 43–57.

Stockar R, Adatte T, Baumgartner PO and Föllmi KB (2013) Palaeoenvironmental significance of organic facies and stable isotope signatures: the Ladinian San Giorgio Dolomite and Meride Limestone of Monte San Giorgio (Switzerland, WHL UNESCO). *Sedimentology* **60**, 239–69.

Sun ZY (2006) *The Middle and Upper Triassic biostratigraphy in western Guizhou and eastern Yunnan*. Ph.D. thesis, Peking University, Beijing, China. Published thesis.

Sun ZY, Hao WC and Jiang DY (2005) Conodont biostratigraphy near the Ladinain-Carnian boundary interval in Guanling of Guizhou. *Journal of Stratigraphy* **29**, 257–63.

Sun ZY, Jiang DY, Ji C and Hao WC (2016) Integrated biochronology for Triassic marine vertebrate faunas of Guizhou Province, South China. *Journal of Asian Earth Sciences* **118**, 101–10.

Sun YD, Joachimski MM, Wignall PB, Yan CB, Chen YL, Jiang HS, Wang LN and Lai XL (2012) Lethally hot temperatures during the Early Triassic Greenhouse. *Science* **338**, 366–70.

Sun YD, Orchard MJ, Kocsis ÁT and Joachimski MM (2020) Carnian–Norian (Late Triassic) climate change: evidence from conodont oxygen isotope thermometry with implications for reef development and Wrangellian tectonics. *Earth and Planetary Science Letters* **534**, 116082. doi: 10.1016/j.epsl.2020.116082.

Sun YD, Richoz S, Krystyn L, Grasby SE, Chen YL, Banerjee D and Joachimski MM (2021) Integrated bio-chemostratigraphy of Lower and Middle Triassic marine successions at Spiti in the Indian Himalaya: implications for the Early Triassic nutrient crisis. *Global and Planetary Change* **196**, 103363. doi: 10.1016/j.gloplacha.2020.103363.

Sun YD, Richoz S, Krystyn L, Zhang ZT and Joachimski MM (2019) Perturbations in carbon cycle during the Carnian Humid Episode: carbonate carbon isotope records from southwestern China and northern Oman. *Journal of the Geological Society, London* **176**, 167–77.

Sun YD, Wignall PB, Joachimski MM, Bond DPG, Grasby SE, Lai XL, Wang LN, Zhang ZT and Sun S (2016) Climate warming, euxinia and carbon isotope perturbations during the Carnian (Triassic) Crisis in South China. *Earth and Planetary Science Letters* **444**, 88–100.

Sweet WC, Mosher LC, Clark D, Collinson JW and Hasenmueller WA (1971) Conodont biostratigraphy of the Triassic. In *Symposium on Conodont Biostratigraphy* (eds WC Stweet and SM Bergstrom), pp. 441–66. Geological Society of America Memoirs no. 127.

Tackett LS (2016) Late Triassic durophagy and the origin of the Mesozoic marine revolution *Palaios* **31**, 122–4.

Tanner LH (2018) *The Late Triassic World: Earth in a Time of Transition.* Cham: Springer.

Tian CR, Dai JY and Tian SG (1983) Triassic conodonts. In *Paleontological Atlas of Southwest China, Volume of Microfossils* (ed. Chendu Institute of Geology and Mineral Resources), pp. 345–98. Beijing: Geological Publishing House.

Tomimatsu Y, Nozaki T, Sato H, Takaya Y, Kimura J-I, Chang Q, Naraoka H, Rigo M and Onoue T (2021) Marine osmium isotope record during the Carnian "pluvial episode" (Late Triassic) in the pelagic Panthalassa Ocean. *Global and Planetary Change* **197**, 103387. doi: 10.1016/j.gloplacha.2020.103387.

Tong JN, Chu DL, Liang L, Shu WC, Song HJ, Song T, Song HY and Wu YY (2019) Triassic integrative stratigraphy and timescale of China. *Science China Earth Sciences* **62**, 189–222.

Trotter JA, Williams IS, Nicora A, Mazza M and Rigo M (2015) Long-term cycles of Triassic climate change: a new δ^{18}O record from conodont apatite. *Earth and Planetary Science Letters* **415**, 165–74.

Vermeij GJ (1977) The Mesozoic marine revolution: evidence from snails, predators and grazers. *Paleobiology* **3**, 245–58.

Wang YG (1983) Ammonoids from Falang Formation (Ladinain-E. Carnian) of southwestern Guizhou, China. *Acta Palaeontologica Sinica* **22**, 153–62.

Wang XF, Bachmann GH, Hagdorn H, Sander PM, Cuny G, Chen XH, Wang CS, Chen LD, Cheng L and Meng FS (2008) The Late Triassic black shales of the Guanling Area, Guizhou Province, South-West China: a unique marine reptile and pelagic crinoid fossil lagerstätte. *Palaeontology* **51**, 27–61.

Wang ZH and Dai JY (1981) Triassic conodonts from the Jiangyou-Beichuan area, Sichuan province. *Acta Palaeotologica Sinica* **20**, 138–52.

Wang CY, Kang PQ and Wang ZH (1998) Conodont-based age of the *Kueichousaurus* Hui Yang, 1958. *Acta Micropalaeotologica Sinica* **15**, 196–8.

Wang CY and Wang ZH (2016) *Conodont Biostratigraphy in China.* Hangzhou: Zhejiang University Press (in Chinese).

Wang HM, Wang XL, Li RX and Wei JY (2005) Triassic conodont succession and stage subdivision of the Guandao section, Bianyang, Luodian, Guizhou. *Acta Palaeontologica Sinica* **44**, 611–26.

Xu GH, Niu ZJ and Chen LD (2003) Triassic cephalopods from the Zhuganpo and Xiaowa Formations in Guanling, Guizhou, with a discussion on the age of the Guanling biota. *Geological Bulletin of China* **22**, 254–65.

Yamashita D, Kato H, Onoue T and Suzuki N (2018) Integrated Upper Triassic conodont and radiolarian biostratigraphies of the Panthalassa Ocean. *Paleontological Research* **22**, 167–97.

Yang SR, Hao WC and Jiang DY (2002) Conodonts of the Fanglang Formation from Langdai, Liuzhi county, Guizhou Province and their age significance. *Geological Review* **48**, 586–92.

Yang SR, Hao WC and Wang XP (1999) Triassic conodont sequences from different facies in China. In *Biotic and Geological Development of the Paleo-Tethys in China* (eds A Yao, Y Ezaki, WC Hao and XP Wang), pp. 97–112. Beijing: Peking University Press.

Yang SR, Liu J and Zhang MF (1995) Conodonts from the Falang Formation of southwestern Guizhou and their age. *Journal of Stratigraphy* **19**, 161–70.

Yao LC (1987) Triassic conodont-bearing Strata in China. *Journal of Tongji University* **15**, 489–99.

Yin HF and Peng YQ (2000) The Triassic of China and its interregional correlation. *Developments in Palaeontology and Stratigraphy* **18**, 197–220.

Zhang L, Orchard MJ, Algeo TJ, Chen Z-Q, Lyu Z, Zhao L, Kaiho K, Ma B and Liu S (2019) An intercalibrated Triassic conodont succession and carbonate carbon isotope profile, Kamura, Japan. *Palaeogeography, Palaeoclimatology, Palaeoecology* **519**, 65–83.

Zhang ZT, Sun YD and Lai XL (2018a) Progresses on Carnian (Late Triassic) conodont study in southwestern China. *Earth Science* **43**, 3955–75.

Zhang ZT, Sun YD, Lai XL, Joachimski MM and Wignall PB (2017) Early Carnian conodont fauna at Yongyue, Zhenfeng area and its implication for Ladinian-Carnian subdivision in Guizhou, South China. *Palaeogeography, Palaeoclimatology, Palaeoecology* **486**, 142–57.

Zhang ZT, Sun YD, Lai XL and Wignall PB (2018b) Carnian (Late Triassic) conodont faunas from southwestern China and their implications. *Papers in Palaeontology* **4**, 513–35.

Zou XD, Balini M, Jiang D, Tintori A, Sun Z and Sun Y (2015) Ammonoids from the Zhuganpo member of the Falang Formation at Nimaigu and their relevance for dating the Xingyi fossil- Lagerstatte (Late Ladinian, Guizhou, China). *Rivista Italiana di Paleontologia e Stratigrafia* **121**, 135–61.